NASA TECHNICAL NOTE

NASA TN D-4283

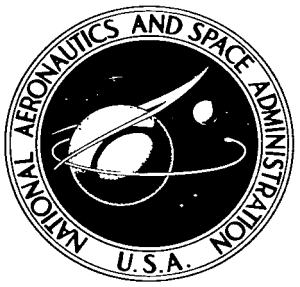

NASA TN D-4283

INFLUENCE OF DISCRETE RING STIFFENERS AND PREBUCKLING DEFORMATIONS ON THE BUCKLING OF ECCENTRICALLY STIFFENED ORTHOTROPIC CYLINDERS

by David L. Block

Langley Research Center
Langley Station, Hampton, Va.

NATIONAL AERONAUTICS AND SPACE ADMINISTRATION • WASHINGTON, D. C. • JANUARY 1968

INFLUENCE OF DISCRETE RING STIFFENERS AND PREBUCKLING DEFORMATIONS ON THE BUCKLING OF ECCENTRICALLY STIFFENED ORTHOTROPIC CYLINDERS

By David L. Block

Langley Research Center
Langley Station, Hampton, Va.

NATIONAL AERONAUTICS AND SPACE ADMINISTRATION

For sale by the Clearinghouse for Federal Scientific and Technical Information
Springfield, Virginia 22151 – CFSTI price $3.00

INFLUENCE OF DISCRETE RING STIFFENERS AND PREBUCKLING DEFORMATIONS ON THE BUCKLING OF ECCENTRICALLY STIFFENED ORTHOTROPIC CYLINDERS*

By David L. Block
Langley Research Center

SUMMARY

The buckling of eccentrically stiffened perfect orthotropic cylinders is the subject of an analytical investigation in which prebuckling deformations and the influence of discretely located ring stiffeners are taken into account. By using energy principles, nonlinear prebuckling equations and linear buckling equations are derived. Solutions for simply supported and clamped boundary conditions and for loadings of axial compression and internal or external pressure are obtained by the method of finite differences and a modified Gaussian elimination technique. For comparative purposes solutions are also presented for the case where the ring properties are averaged and a Galerkin solution is presented for the classical buckling (constant prebuckling deformations) of a simply supported cylinder with discrete rings. Computed results for two types of simply supported large-diameter stiffened cylinders loaded in axial compression illustrate the influence on the buckling load of prebuckling deformations, discrete rings, and eccentricity of applied axial compressive loads; results for clamped longitudinally stiffened cylinders are compared with previous test results.

The results show that the predicted buckling load may be substantially affected by consideration of prebuckling deformations, eccentric loading, and discreteness of rings and that agreement with experiment may be improved by including these factors.

INTRODUCTION

In the design of lightweight structures, an understanding of the various effects of stiffening elements on the buckling behavior of cylindrical shells is important. The importance of one of these effects, the eccentricity or one-sidedness of stiffening elements, on the buckling strength has been demonstrated in several studies. (See

*The information presented herein is based upon a thesis offered in partial fulfillment of the requirements for the degree of Doctor of Philosophy in Engineering Mechanics, Virginia Polytechnic Institute, Blacksburg, Virginia, June 1966.

refs. 1 to 8.) However, differences between experiment and theory (ref. 7) show a need for additional considerations in the theories, such as prebuckling deformations, discrete stiffeners, initial imperfections, and boundary conditions.

The importance of prebuckling deformations has been demonstrated for unstiffened isotropic cylinders in references 9 and 10 and for stiffened isotropic cylinders in reference 6. In reference 6, however, only simple supports are considered and an approximate one-mode Galerkin solution is used to obtain the buckling loads. The importance of discrete rings has been studied in reference 11 for simply supported orthotropic cylinders in axial compression, but the theory used did not consider eccentricities of stiffeners or prebuckling deformations. In reference 5 a discrete-ring theory is presented for stiffened isotropic cylinders but prebuckling deformations are neglected.

The purpose of this paper is to present a theoretical investigation of the effects of both prebuckling deformations and stiffener discreteness on buckling of eccentrically stiffened cylinders. The effect of discrete stiffeners is studied only for rings because in stiffened cylinders of practical size, the longitudinal stiffeners or stringers are closely spaced and therefore can be assumed to be averaged or "smeared out" over the stringer spacing. The cylinders studied are assumed to have simply supported or clamped boundary conditions and to be loaded by axial compression and a constant pressure. Also investigated is the influence of eccentricity of the applied axial loads; that is, the effect of applying the axial-load resultant at a surface other than the cylinder's middle surface. (See, for example, ref. 6.)

The analysis presented is applicable to a broad class of cylindrical shell structures, because the shell considered is constructed from orthotropic material with stiffening elements on its surface. By proper definition of the orthotropic material constants such an analysis can be used to predict buckling for a wide variety of stiffened shells – for example, sandwich-type, corrugated, filament-wound, or isotropic cylinders.

Nonlinear prebuckling equations and boundary conditions and linear buckling equations and boundary conditions are derived for cylinders with discrete rings (appendix A). Solutions to the prebuckling and buckling equations are obtained for simply supported and clamped boundary conditions by the method of finite differences and a modified Gaussian elimination procedure. (See, for example, refs. 12 and 13.) For comparison, solutions are also presented for cylinders with rings that are considered to be smeared out (appendix B), and for the classical buckling problem of a simply supported cylinder with discrete rings and a membrane stress state prior to buckling (appendix C). Because of the large number of parameters involved in the problem, results of a general nature are impractical to present; thus, results in the form of sample calculations are presented for two large-diameter axially compressed simply supported cylinders, and for clamped

longitudinally stiffened cylinders of the same proportions as the test cylinders of reference 7.

SYMBOLS

A	cross-sectional area of stiffener
A_i, B_i, C_i $\bar{A}, \bar{B}, \bar{C}$	4×4 matrices defined in appendix D
D_x, D_y	bending stiffness of orthotropic plate in longitudinal and circumferential directions, respectively
$\bar{D}_x$	longitudinal bending-stiffness parameter, $\frac{D_x}{1 - \mu_x \mu_y} + \frac{E_s I_s}{d} + \frac{E_s A_s \bar{z}_s^2}{d}$
D_{xy}	twisting stiffness of orthotropic plate
E	Young's modulus
E_x, E_y	extensional stiffness of orthotropic plate in longitudinal and circumferential directions, respectively (for corrugated cylinders see ref. 8)
$\bar{E}_x$	longitudinal extensional-stiffness parameter, $\frac{E_x}{1 - \tilde{\mu}_x \tilde{\mu}_y} + \frac{E_s A_s}{d}$
$F_1, F_2, \ldots, F_{11}$	constants defined in appendix D
G	shear modulus
G_{xy}	in-plane shear stiffness of orthotropic plate
I	moment of inertia of stiffener about its centroid
I_o	moment of inertia of stiffener about middle surface of shell
J	torsional constant for stiffener
$\bar{K}, \bar{L}$	matrices defined by equations (28)

L_i	matrix defined by equation (27b)
M	buckling-moment function of x defined by equation (35)
M_x, M_y, M_{xy}	middle-surface moment resultants for stiffened shell
$\bar{M}_x, \bar{M}_y, \bar{M}_{xy}$	middle-surface moment resultants for orthotropic shell
N_x, N_y, N_{xy}	middle-surface stress resultants for stiffened shell
$\bar{N}_x, \bar{N}_y, \bar{N}_{xy}$	middle-surface stress resultants for orthotropic shell
$\hat{N}_x$	magnitude of externally applied axial compressive load
N	total number of rings on cylinder
P_i	4×4 recurrence-relation matrices defined by equations (44) and (45)
$\bar{P}_i, \bar{Q}_i$	recurrence-relation matrices defined by equations (31) and (33)
R	radius of cylinder to middle surface of orthotropic shell (see fig. 1)
S	matrix defined by equation (27c)
$\bar{S}$	matrices defined by equation (28)
U,V,W	buckling-displacement functions of x defined by equations (35)
$Z_A = \begin{Bmatrix} \xi \\ w_A \end{Bmatrix}$	
$Z_B = \begin{Bmatrix} U \\ V \\ W \\ M \end{Bmatrix}$	
a	length of stiffened cylinder (see fig. 1)
a_q, b_q, c_q	series coefficients of equations (C4)

a_r, b_r, c_r	series coefficients of equations (C6)
d	stringer spacing (see fig. 1)
$\bar{e}$	distance from middle surface of cylinder to line on which $\hat{N}_x$ acts
h	one-half the height of the stringer section (see fig. 2(b))
j	integer
k	total number of finite-difference stations along length of cylinder
l	ring spacing (see fig. 1)
m	number of finite-difference spaces Δ between adjacent rings
n	number of full waves in cylinder buckle pattern in circumferential direction
p	pressure (positive for external pressure)
q,r,s	integers
t	thickness of isotropic-cylinder shell wall
$\bar{t}$	effective wall thickness of stiffened isotropic cylinder, $\frac{A_s}{d} + t$
u,v,w	middle-surface displacements of orthotropic shell in x-, y-, and z-directions, respectively
x,y,z	orthogonal curvilinear coordinates with origin lying in middle surface of orthotropic shell (see fig. 1)
$\bar{z}$	distance from centroid of stiffener to middle surface of orthotropic shell (see fig. 1), positive if stiffener lies on external surface of shell
α_1, α_2	constants defined by equations (B3)
$\bar{\alpha}$	4×4 selection matrix defined in appendix D

$\beta_1,\beta_2,\ldots,\beta_6$ constants defined by equations (9) and (23)

$\gamma_1,\gamma_2,\gamma_3,\gamma_4$ constants defined by equations (B3), (B4), and (B5)

γ_{xy} shearing strain at middle surface of orthotropic shell

γ_{xy_T} shearing strain in orthotropic shell

Δ distance between adjacent finite-difference stations

$\delta(x-j\ell)$ Dirac delta function defined so that $\int_{-\infty}^{+\infty} f(x)\delta(x-j\ell)dx = f(j\ell)$, where $\delta(x-j\ell) = 0$ when $x \neq j\ell$

δ_{ij} Kronecker delta, equal to 0 when $i \neq j$ and equal to 1 when $i = j$

ϵ_x,ϵ_y normal strains at middle surface of orthotropic shell

$\epsilon_{x_T},\epsilon_{y_T}$ normal strains in orthotropic shell

$\epsilon_{y_r},\epsilon_{x_s}$ strain in rings and stringers, respectively

κ constant defined by equation (B3)

$\Lambda_1,\Lambda_2,\ldots,\Lambda_{24}$ constants defined in appendix D

μ_x,μ_y Poisson's ratios for bending of orthotropic plate in longitudinal and circumferential directions, respectively

$\tilde{\mu}_x,\tilde{\mu}_y$ Poisson's ratios for extension of orthotropic plate in longitudinal and circumferential directions, respectively

$\xi = w_A''$

Π total potential energy of stiffened cylinder

Π_c strain energy of orthotropic shell

Π_L potential energy of external forces

Π_r, Π_s strain energy of rings and stringers, respectively

Φ_r, Φ_{rq}
Ψ_r, Ψ_{rq} } trigonometric series defined by equations (C8)

Subscripts:

A prebuckling state

B small changes away from prebuckling state which occur at buckling

H integer denoting finite-difference station at which ring is located (see eq. (19))

i index of finite-difference station

max maximum

r rings (circumferential stiffening)

s stringers (longitudinal stiffening)

A subscript preceded by a comma indicates partial differentiation with respect to the subscript.

Primes indicate total derivatives with respect to x.

GOVERNING EQUATIONS AND BOUNDARY CONDITIONS

To develop the buckling theory for the stiffened cylinder, shown in figure 1, several basic assumptions are made. The stiffened cylinder is composed of an orthotropic shell stiffened by uniform, equally spaced rings and stringers, all having elastic properties. The elastic constants of the orthotropic shell are taken as those given in reference 14, with the assumption that the transverse shearing stiffnesses of the shell are infinitely large. The stringers are assumed to be closely spaced so that their elastic properties can be averaged over the stringer spacing. However, the rings are considered to be located discretely along circumferential lines on the cylinder. In cases where rings and stringers lie on the same surface of the shell, the effect of the joints in the stiffener

framework is ignored. The only applied loadings considered are an axial compressive end load and a constant pressure load.

The equations are derived by obtaining strain-energy expressions for the shell, stiffeners, and loadings and applying the method of minimum potential energy to obtain the nonlinear equilibrium equations and boundary conditions of the configuration. This derivation is presented in appendix A and is similar to the derivation presented in reference 4 except that orthotropic constitutive relations are employed for the shell and the rings are treated as discrete members.

The nonlinear equilibrium equations which govern an eccentrically stiffened orthotropic cylinder with discrete rings are

$$\left.\begin{aligned} &N_{x,x} + N_{xy,y} = 0 \\ &N_{y,y} + N_{xy,x} = 0 \\ &-M_{x,xx} + M_{xy,xy} - M_{y,yy} + \frac{N_y}{R} - N_x w_{,xx} - N_y w_{,yy} - 2N_{xy} w_{,xy} + p = 0 \end{aligned}\right\} \tag{1}$$

where a comma denotes partial differentiation with respect to the subscript. The boundary conditions to be satisfied at each end of the cylinder are

$$\left.\begin{aligned} &N_x + \hat{N}_x = 0 && \text{or} \quad u = 0 \\ &N_{xy} = 0 && \text{or} \quad v = 0 \\ &M_x + \hat{N}_x \bar{e} = 0 && \text{or} \quad w_{,x} = 0 \\ &M_{x,x} - M_{xy,y} + N_x w_{,x} + N_{xy} w_{,y} = 0 && \text{or} \quad w = 0 \end{aligned}\right\} \tag{2}$$

The stress and moment resultants in equations (1) and (2) are given by equations (A14) in appendix A.

The nonlinear equilibrium equations and boundary conditions (eqs. (1) and (2)) are used to obtain the equations and boundary conditions which govern the prebuckling and buckling of a stiffened cylinder with discrete rings. To obtain the prebuckling and buckling equations, the displacements of the shell u, v, and w are assumed to be separable into two parts as follows:

$$\left.\begin{aligned} u(x,y) &= u_A(x) + u_B(x,y) \\ v(x,y) &= v_A(x) + v_B(x,y) \\ w(x,y) &= w_A(x) + w_B(x,y) \end{aligned}\right\} \tag{3}$$

The first part, denoted by the subscript A, is an axisymmetric prebuckling displacement. The second part, denoted by B, is the infinitesimal nonaxisymmetric displacement that occurs at buckling.

Prebuckling Equations

The equilibrium equations which govern the axisymmetric prebuckling are obtained from substitution of the axisymmetric displacement in equations (3) into equations (1) and are found to be

$$\left.\begin{aligned} N'_{x_A} &= 0 \\ N'_{xy_A} &= 0 \\ -M''_{x_A} + \frac{N_{y_A}}{R} - N_{x_A} w''_A + p &= 0 \end{aligned}\right\} \tag{4}$$

where the primes denote total differentiation with respect to x.

The appropriate set of boundary conditions is found similarly from equations (2) to be

$$\left.\begin{aligned} N_{x_A} + \hat{N}_x = 0 \quad &\text{or} \quad u_A = 0 \\ N_{xy_A} = 0 \quad &\text{or} \quad v_A = 0 \\ M_{x_A} + \hat{N}_x \bar{e} = 0 \quad &\text{or} \quad w'_A = 0 \\ M'_{x_A} + N_{x_A} w'_A = 0 \quad &\text{or} \quad w_A = 0 \end{aligned}\right\} \tag{5}$$

In equations (4) and (5),

$$N_{x_A} = \frac{E_x}{1 - \tilde{\mu}_x\tilde{\mu}_y}\left[u'_A + \frac{1}{2}\left(w'_A\right)^2 + \tilde{\mu}_y\frac{w_A}{R}\right] + \frac{E_sA_s}{d}\left[u'_A + \frac{1}{2}\left(w'_A\right)^2 - \bar{z}_s w''_A\right] \tag{6a}$$

$$N_{y_A} = \frac{E_y}{1 - \tilde{\mu}_x\tilde{\mu}_y}\left\{\frac{w_A}{R} + \tilde{\mu}_x\left[u'_A + \frac{1}{2}\left(w'_A\right)^2\right]\right\} + \sum_{j=1}^{N}\delta(x-j\ell)E_rA_r\frac{w_A}{R} \tag{6b}$$

$$N_{xy_A} = G_{xy}v'_A \tag{6c}$$

$$M_{x_A} = -\left\{\left(\frac{D_x}{1 - \mu_x\mu_y} + \frac{E_sI_{o_s}}{d}\right)w''_A - \frac{E_sA_s\bar{z}_s}{d}\left[u'_A + \frac{1}{2}\left(w'_A\right)^2\right]\right\} \tag{6d}$$

The first of equations (4) and (5) require that N_{x_A} = Constant = $-\hat{N}_x$. The second of equations (4) and (5) require that N_{xy_A} = Constant = 0 (no applied shear). From equations (6a) and (6b) together with $N_{x_A} = -\hat{N}_x$, N_{y_A} can be written as

$$N_{y_A} = \frac{E_y\tilde{\mu}_xE_sA_s\bar{z}_s}{\bar{E}_x\left(1 - \tilde{\mu}_x\tilde{\mu}_y\right)d}w''_A + \left[\frac{E_y\left(E_x + \frac{E_sA_s}{d}\right)}{\bar{E}_xR\left(1 - \tilde{\mu}_x\tilde{\mu}_y\right)} + \sum_{j=1}^{N}\delta(x-j\ell)\frac{E_rA_r}{R}\right]w_A - \frac{E_y\tilde{\mu}_x}{\bar{E}_x\left(1 - \tilde{\mu}_x\tilde{\mu}_y\right)}\hat{N}_x \tag{7}$$

where

$$\bar{E}_x = \frac{E_x}{1 - \tilde{\mu}_x\tilde{\mu}_y} + \frac{E_sA_s}{d}$$

The equation determining the prebuckling deflection is now obtained from equations (4), (6), and (7) as

$$\beta_1w''''_A + \beta_2w''_A + \left[\beta_3 + \sum_{j=1}^{N}\delta(x-j\ell)\beta_4\right]w_A - \beta_5 = 0 \tag{8}$$

where

$$\beta_1 = \frac{D_x}{1 - \mu_x\mu_y} + \frac{E_sI_s}{d} + \frac{E_sA_s\bar{z}_s^{\,2}E_x}{\bar{E}_x\left(1 - \tilde{\mu}_x\tilde{\mu}_y\right)d} \tag{9a}$$

$$\beta_2 = \frac{2E_y\tilde{\mu}_x E_s A_s \bar{z}_s}{\bar{E}_x R\left(1 - \tilde{\mu}_x\tilde{\mu}_y\right)d} + \hat{N}_x \tag{9b}$$

$$\beta_3 = \frac{E_y}{\bar{E}_x R^2\left(1 - \tilde{\mu}_x\tilde{\mu}_y\right)}\left(E_x + \frac{E_s A_s}{d}\right) \tag{9c}$$

$$\beta_4 = \frac{E_r A_r}{R^2} \tag{9d}$$

$$\beta_5 = \frac{E_y\tilde{\mu}_x}{\bar{E}_x R\left(1 - \tilde{\mu}_x\tilde{\mu}_y\right)}\hat{N}_x - p \tag{9e}$$

and $I_s = I_{o_s} - A_s\bar{z}_s^2$. The boundary conditions are

$$\left.\begin{aligned} M_{x_A} + \hat{N}_x\bar{e} = 0 \quad &\text{or} \quad w'_A = 0 \\ M'_{x_A} - \hat{N}_x w'_A = 0 \quad &\text{or} \quad w_A = 0 \end{aligned}\right\} \tag{10}$$

The reciprocal relations $\tilde{\mu}_x E_y = \tilde{\mu}_y E_x$ and $\mu_x D_y = \mu_y D_x$ have been employed to simplify the equations.

Buckling Equations

The equilibrium equations and boundary conditions which govern the buckling of a stiffened cylinder with discrete rings are obtained by substituting equations (3) into equations (1) and (2). If only linear terms in the buckling displacements (subscript B terms) are retained, and if identities (4) are subtracted out, the following buckling equations are obtained:

$$\left.\begin{aligned} &N_{x_{B,x}} + N_{xy_{B,y}} = 0 \\ &N_{y_{B,y}} + N_{xy_{B,x}} = 0 \\ &-M_{x_{B,xx}} + M_{xy_{B,xy}} - M_{y_{B,yy}} + \frac{N_{y_B}}{R} - N_{x_A}w_{B,xx} - N_{x_B}w''_A \\ &- N_{y_A}w_{B,yy} - 2N_{xy_A}w_{B,xy} = 0 \end{aligned}\right\} \tag{11}$$

with the boundary conditions

$$\left.\begin{aligned} & N_{x_B} = 0 \quad \text{or} \quad u_B = 0 \\ & N_{xy_B} = 0 \quad \text{or} \quad v_B = 0 \\ & M_{x_B} = 0 \quad \text{or} \quad w_{B,x} = 0 \\ \text{and} \quad & M_{x_{B,x}} - M_{xy_{B,y}} + N_{x_A} w_{B,x} + N_{x_B} w'_A + N_{xy_A} w_{B,y} = 0 \\ & \qquad \text{or} \\ & w_B = 0 \end{aligned}\right\} \tag{12}$$

where

$$N_{x_B} = \frac{E_x}{1 - \tilde{\mu}_x \tilde{\mu}_y}\left[u_{B,x} + w'_A w_{B,x} + \tilde{\mu}_y\left(v_{B,y} + \frac{w_B}{R}\right)\right] + \frac{E_s A_s}{d}\left(u_{B,x} + w'_A w_{B,x} - \bar{z}_s w_{B,xx}\right) \tag{13a}$$

$$N_{y_B} = \frac{E_y}{1 - \tilde{\mu}_x \tilde{\mu}_y}\left[v_{B,y} + \frac{w_B}{R} + \tilde{\mu}_x\left(u_{B,x} + w'_A w_{B,x}\right)\right] + \sum_{j=1}^{N} \delta(x - j\ell) E_r A_r \left(v_{B,y} + \frac{w_B}{R} - \bar{z}_r w_{B,yy}\right) \tag{13b}$$

$$N_{xy_B} = G_{xy}\left(u_{B,y} + v_{B,x} + w'_A w_{B,y}\right) \tag{13c}$$

$$M_{x_B} = -\left[\frac{D_x}{1 - \mu_x \mu_y}\left(w_{B,xx} + \mu_y w_{B,yy}\right) + \frac{E_s I_s}{d} w_{B,xx} - \frac{E_s A_s \bar{z}_s}{d}\left(u_{B,x} + w'_A w_{B,x} - \bar{z}_s w_{B,xx}\right)\right] \tag{13d}$$

$$M_{y_B} = -\left\{\frac{D_y}{1 - \mu_x\mu_y}\left(w_{B,yy} + \mu_x w_{B,xx}\right)\right.$$

$$\left. + \sum_{j=1}^{N} \delta(x-j\ell)\left[E_r I_r w_{B,yy} - E_r A_r \bar{z}_r\left(v_{B,y} + \frac{w_B}{R} - \bar{z}_r w_{B,yy}\right)\right]\right\} \tag{13e}$$

$$M_{xy_B} = \left[2D_{xy} + \frac{G_s J_s}{d} + \sum_{j=1}^{N} \delta(x-j\ell) G_r J_r\right] w_{B,xy} \tag{13f}$$

and

$$I_r = I_{o_r} - A_r \bar{z}_r^2$$

To solve the buckling equations (11) and apply boundary conditions (12), the prebuckling quantities (subscript A) must first be determined by solution of the prebuckling equation (8) and boundary conditions (10). The solution of the prebuckling and buckling equations is discussed in the next section.

SOLUTIONS

In this section solutions of the prebuckling and buckling equations are obtained for simply supported and clamped shells by use of the finite-difference method. The prebuckling and buckling equations are solved by employing a technique in which the system of governing differential equations is changed to a system of second-order differential equations and then these equations are written in terms of finite differences. The resulting difference equations are then written in matrix form and solved by a modified Gaussian elimination technique. Details of the solutions follow.

Solution of Prebuckling Equations

The governing equation for the prebuckling displacement, equation (8), is a fourth-order, variable-coefficient, ordinary differential equation and is changed to a system of second-order differential equations by letting

$$\xi = w_A'' \tag{14}$$

Now equation (8) can be written as

$$\beta_1 \xi'' + \beta_2 \xi + \left[\beta_3 + \sum_{j=1}^{N} \delta(x-j\ell)\beta_4\right] w_A - \beta_5 = 0 \tag{15}$$

The terms β_1 to β_5 are defined by equations (9). Equations (14) and (15) are now the governing equations for the prebuckling displacements.

When the derivatives occurring in equations (14) and (15) are replaced by finite differences, a set of simultaneous linear algebraic equations for the values of w_A and ξ at discrete points along the length of the cylinder is obtained. The stations along the length of the cylinder are taken to be equally spaced and are numbered from $i = 0$ at one end of the cylinder (at $x = 0$) to $i = k$ at the other end of the cylinder (at $x = a$). The following central-difference approximations for the first and second derivatives are used:

$$\left.\begin{aligned} (f')_i &= \frac{f_{i+1} - f_{i-1}}{2\Delta} \\ (f'')_i &= \frac{f_{i+1} - 2f_i + f_{i-1}}{\Delta^2} \end{aligned}\right\} \tag{16}$$

where i indicates the station and Δ is the distance between adjacent stations. As a consequence of employing central differences, there are also stations corresponding to $i = -1$ and $i = k + 1$. When equations (16) are substituted, equations (14) and (15) for $i = 1, 2, \ldots, k - 1$ become

$$\left.\begin{aligned} &\beta_1 \frac{\xi_{i+1} - 2\xi_i + \xi_{i-1}}{\Delta^2} + \beta_2 \xi_i + \left(\beta_3 + \frac{\delta_{iH}\beta_4}{\Delta}\right) w_{A_i} - \beta_5 = 0 \\ &\frac{w_{A_{i+1}} - 2w_{A_i} + w_{A_{i-1}}}{\Delta^2} - \xi_i = 0 \end{aligned}\right\} \tag{17}$$

where

$$\left.\begin{aligned} \delta_{iH} &= 1 \qquad (i = H) \\ \delta_{iH} &= 0 \qquad (i \neq H) \end{aligned}\right\} \tag{18}$$

The subscript H denotes the difference station at which a ring is located and can be expressed as

$$H = mj \qquad (j = 1, 2, \ldots, N) \tag{19}$$

where m is the number of difference spaces Δ between adjacent rings and N is the total number of rings on the cylinder as previously defined. Note in equations (17) that the finite-difference procedure requires that the ring properties be averaged (or smeared out) over one difference spacing Δ. At each of the stations, ξ_i and w_{A_i} are unknowns; hence, the total number of unknowns is $2(k + 1)$. Equations (17) represent $2(k - 1)$ equations. The boundary conditions yield the four additional equations that are needed to give $2(k + 1)$ equations and $2(k + 1)$ unknowns.

From equations (10), with the assumption that the shell has the same boundary conditions at each end and is supported at the ends, the prebuckling boundary conditions at $x = 0$ and $x = a$ are

$$\left.\begin{aligned} w_A &= 0 \\ M_{x_A} + \hat{N}_x \bar{e} &= 0 \quad \text{or} \quad w'_A = 0 \end{aligned}\right\} \tag{20}$$

By using equations (6), (14), and (16), these boundary conditions can be written in terms of finite differences at stations $i = 0$ and $i = k$ (at the ends of the cylinder, $x = 0$ and $x = a$, respectively) as follows:

$$\left.\begin{aligned} w_{A_0} &= 0 \\ w_{A_k} &= 0 \end{aligned}\right\} \tag{21}$$

For simply supported shells,

$$\left.\begin{aligned} \xi_0 &= \frac{\beta_6}{\beta_1} \\ \xi_k &= \frac{\beta_6}{\beta_1} \end{aligned}\right\} \tag{22a}$$

and for clamped shells,

$$\left.\begin{aligned} \Delta^2\xi_0 - 2wA_1 + 2wA_0 &= 0 \\ \Delta^2\xi_k - 2wA_{k-1} + 2wA_k &= 0 \end{aligned}\right\} \tag{22b}$$

In equations (22a),

$$\beta_6 = \hat{N}_x\left(\bar{e} - \frac{E_S A_S \bar{z}_S}{\bar{E}_x d}\right) \tag{23}$$

and β_1 is as defined by equation (9a).

The governing difference equations (17) and boundary conditions (21) and (22) will now be solved by a matrix technique. Equations (17) can be written in matrix form as

$$Z_{A_{i-1}} + L_i Z_{A_i} + Z_{A_{i+1}} = S \qquad (i = 1, 2, \ldots, k-1) \tag{24}$$

and equations (21) and (22) as

$$\bar{K} Z_{A_1} + \bar{L} Z_{A_0} = \bar{S} \tag{25}$$

$$\bar{\bar{K}} Z_{A_{k-1}} + \bar{\bar{L}} Z_{A_k} = \bar{\bar{S}} \tag{26}$$

where

$$Z_{A_i} = \begin{Bmatrix} \xi_i \\ wA_i \end{Bmatrix} \tag{27a}$$

$$L_i = \begin{bmatrix} \left(-2 + \dfrac{\Delta^2\beta_2}{\beta_1}\right) & \left(\dfrac{\Delta^2\beta_3}{\beta_1} + \dfrac{\Delta\beta_4\delta_{iH}}{\beta_1}\right) \\ -\Delta^2 & -2 \end{bmatrix} \tag{27b}$$

$$S = \begin{Bmatrix} \dfrac{\Delta^2 \beta_5}{\beta_1} \\ 0 \end{Bmatrix} \tag{27c}$$

For simply supported boundary conditions,

$$\bar{K} = \begin{bmatrix} 0 & 0 \\ 0 & 0 \end{bmatrix} \qquad \bar{L} = \begin{bmatrix} 1 & 0 \\ 0 & 1 \end{bmatrix} \qquad \bar{S} = \begin{Bmatrix} \dfrac{\beta_6}{\beta_1} \\ 0 \end{Bmatrix} \tag{28a}$$

and for clamped boundary conditions,

$$\bar{K} = \begin{bmatrix} 0 & -2 \\ 0 & 0 \end{bmatrix} \qquad \bar{L} = \begin{bmatrix} \Delta^2 & 2 \\ 0 & 1 \end{bmatrix} \qquad \bar{S} = \begin{Bmatrix} 0 \\ 0 \end{Bmatrix} \tag{28b}$$

The set of matrix equations (24), (25), and (26) is solved by a Gaussian elimination technique which has been formalized in reference 15. This method proceeds as follows: The first of equations (24) together with equation (25) is solved for Z_{A_1} in terms of Z_{A_2}; this result is substituted into the next of equations (24) and Z_{A_2} is found in terms of Z_{A_3}, and so on. Finally, the last of equations (24) together with equation (26) determines $Z_{A_{k-1}}$, and then all of the Z_{A_i} are calculated in reverse order. In the procedure just described, it follows from the first of equations (24) and equation (25) that

$$Z_{A_1} = \left[L_1 - \bar{L}^{-1}\bar{K}\right]^{-1}\left[-Z_{A_2} + S - \bar{S}\bar{L}^{-1}\right] \tag{29}$$

Now the general result for Z_{A_i} can be written in terms of $Z_{A_{i+1}}$ as

$$Z_{A_i} = \bar{P}_i Z_{A_{i+1}} + \bar{Q}_i \tag{30}$$

From equation (29) and equation (30) for $i = 1$, $\bar{P}_1$ and $\bar{Q}_1$ can be determined as

$$\left.\begin{aligned} \bar{P}_1 &= -\left[L_1 - \bar{L}^{-1}\bar{K}\right]^{-1} \\ \bar{Q}_1 &= \left[L_1 - \bar{L}^{-1}\bar{K}\right]^{-1}\left[S - \bar{S}\bar{L}^{-1}\right] \end{aligned}\right\} \tag{31}$$

The substitution of $Z_{A_{i-1}} = \bar{P}_{i-1}Z_{A_i} + \bar{Q}_{i-1}$ into the general equation (24) gives

$$Z_{A_i} = \left[\bar{P}_{i-1} + L_i\right]^{-1}\left[-Z_{A_{i+1}} + S - \bar{Q}_{i-1}\right] \qquad (i = 2, 3, \ldots, k-1) \tag{32}$$

Thus

$$\left.\begin{aligned} \bar{P}_i &= -\left[\bar{P}_{i-1} + L_i\right]^{-1} \\ \bar{Q}_i &= \left[\bar{P}_{i-1} + L_i\right]^{-1}\left[S - Q_{i-1}\right] \end{aligned}\right\} \quad (i = 2, 3, \ldots, k-1) \tag{33}$$

where $\bar{P}_1$ and $\bar{Q}_1$ are given by equations (31). The recurrence-relation equations (33) provide all the $\bar{P}_i$ and $\bar{Q}_i$ up to $\bar{P}_{k-1}$ and $\bar{Q}_{k-1}$. By using equations (26) and (30), $Z_{A_{k-1}}$ can be found explicitly as

$$Z_{A_{k-1}} = \left[\bar{I} + \bar{P}_{k-1}\bar{L}^{-1}\bar{K}\right]^{-1}\left[\bar{P}_{k-1}\bar{S} + \bar{Q}_{k-1}\right] \tag{34}$$

where

$$\bar{I} = \begin{bmatrix} 1 & 0 \\ 0 & 1 \end{bmatrix}$$

Now $Z_{A_{k-2}}, Z_{A_{k-3}}, \ldots, Z_{A_1}$ can be determined from equation (30). For this solution the only matrix inversions for the Z_{A_i} are of 2×2 matrices; therefore the solution is well adapted for rapid computer calculation. Once the Z_{A_i} have been calculated, the prebuckling displacements w_A at any station along the cylinder are known.

Solution of Buckling Equations

The buckling load of a stiffened orthotropic cylinder with discrete rings can be obtained by solving the previously developed buckling equations (11) along with boundary

conditions (12). In equations (11) and (12), the conditions of continuity around the cylinder are satisfied if

$$\left.\begin{aligned} u_B &= U(x)\cos\frac{ny}{R} \\ v_B &= V(x)\sin\frac{ny}{R} \\ w_B &= W(x)\cos\frac{ny}{R} \\ M_{x_B} &= M(x)\cos\frac{ny}{R} \end{aligned}\right\} \tag{35}$$

where n, the number of circumferential waves, is an integer. The buckling equations (11) may now be converted to ordinary differential equations with variable coefficients. The variable M is included as an explicit dependent variable because the eighth-order system of differential equations will be expressed for convenience, as four second-order equations in u, v, w, and M. By making this change the finite-difference method of solution previously described for the prebuckling equation can be employed.

In buckling equations (11), one additional step has to be performed in order to prevent the appearance of derivatives of x of higher order than two. A higher order derivative in w_B will appear when the N_{x_B} term is differentiated in the first of equations (11). This higher order derivative is eliminated as follows: Equation (13d) is solved for $w_{B,xx}$ and this result is substituted into equation (13a) to give N_{x_B} in terms of M_{x_B} and derivatives of x of less than second order. In performing this step and in substituting equations (35) and equation (7) for N_{y_A}, the following variable-coefficient second-order ordinary differential equations for the buckling load are obtained:

$$\Lambda_1 U'' - \Lambda_2 U + \Lambda_3 V' + \Lambda_1 w_A' W'' + \left(\Lambda_1 w_A'' + \Lambda_4\right) W' - \Lambda_2 w_A' W + \Lambda_5 M' = 0 \tag{36a}$$

$$-\Lambda_3 U' + \Lambda_6 V'' - \left[\Lambda_7 + \sum_{j=1}^{N} \delta(x-j\ell)\Lambda_8\right] V - \Lambda_3 w_A' W' - \left[\Lambda_9 + \Lambda_{10} w_A'' + \sum_{j=1}^{N} \delta(x-j\ell)\Lambda_{11}\right] W = 0 \tag{36b}$$

$$\left(\Lambda_{12} - \Lambda_{13}w''_A\right)U' + \left[\Lambda_9 - \Lambda_{14}w''_A + \sum_{j=1}^{N} \delta(x-j\ell)\Lambda_{11}\right]V$$

$$+ \left[-\Lambda_{15} + \hat{N}_x + \Lambda_{16}w''_A - \sum_{j=1}^{N} \delta(x-j\ell)\Lambda_{17}\right]W'' + \left[\Lambda_{12}w'_A - \Lambda_{13}w''_A w'_A - \sum_{j=1}^{N} \delta(x-j\ell)'\Lambda_{17}\right]W'$$

$$+ \left[\Lambda_{18} - \Lambda_{19}\hat{N}_x + \Lambda_{20}w''_A + \Lambda_{21}w_A + \sum_{j=1}^{N} \delta(x-j\ell)\left(\Lambda_{22} + \Lambda_{23}w_A\right)\right]W - M'' = 0 \qquad (36c)$$

$$-\Lambda_{16}U' + \bar{D}_x W'' - \Lambda_{16}w'_A W' - \Lambda_{24}W + M = 0 \qquad (36d)$$

where

$$\bar{D}_x = \frac{D_x}{1 - \mu_x\mu_y} + \frac{E_S I_S}{d} + \frac{E_S A_S \bar{z}_S^2}{d}$$

The coefficients Λ_1 to Λ_{24} are given in appendix D. Equation (36d) is obtained from equation (13d).

Writing equations (36) in finite differences at each station along the length of the cylinder, using the same numbering system as in the prebuckling solution and difference equations (16), and then writing the resulting difference equations in matrix form results in the following matrix equation:

$$A_i Z_{B_{i-1}} + B_i Z_{B_i} + C_i Z_{B_{i+1}} = 0 \qquad (i = 0, 1, 2, \ldots, k) \qquad (37)$$

where

$$Z_{B_i} = \begin{Bmatrix} U_i \\ V_i \\ W_i \\ M_i \end{Bmatrix} \qquad (38)$$

and where the 4×4 coefficient matrices A_i, B_i, and C_i are given in appendix D. In writing the matrix difference equations (37), the ring properties are again assumed to be averaged over one difference spacing Δ as in the prebuckling solution. Also, as in the

prebuckling solution, the boundary conditions give the additional equations needed in order to have the same number of unknowns as there are equations.

From equations (12), with the assumption that the shell is supported at the ends, the boundary conditions on the buckling displacements are

$$\left.\begin{array}{lll} N_{x_B} = 0 & \text{or} & u_B = 0 \\ N_{xy_B} = 0 & \text{or} & v_B = 0 \\ & w_B = 0 & \\ M_{x_B} = 0 & \text{or} & w_{B,x} = 0 \end{array}\right\} \tag{39}$$

Equations (39) admit the possibility of eight different sets of boundary conditions (four simple support and four clamped). By substituting equations (35) and writing in finite-difference form, the eight sets of boundary conditions can be written in matrix form at stations $i = 0$ and $i = k$ (at ends of cylinder, $x = 0$ and $x = a$, respectively) as follows:

$$\bar{A}_0 Z_{B_{-1}} + \bar{B}_0 Z_{B_0} + \bar{C}_0 Z_{B_1} = 0 \tag{40}$$

$$\bar{A}_k Z_{B_{k-1}} + \bar{B}_k Z_{B_k} + \bar{C}_k Z_{B_{k+1}} = 0 \tag{41}$$

where Z_B is as defined by equation (38), and $\bar{A}$, $\bar{B}$, and $\bar{C}$ are 4×4 coefficient matrices whose terms depend upon the selected boundary conditions and whose values are given in appendix D.

In the 4×4 matrix coefficient expressions of equations (37), (40), and (41), the prebuckling displacements and derivatives at each station are determined from the prebuckling solution (eqs. (30) to (34), along with the appropriate boundary conditions). The matrix difference equations (37), (40), and (41) define a linear homogeneous system of equations which have a nontrivial solution only if the determinant of the coefficient matrix equals zero. For a specified pressure the lowest value of $\hat{N}_x$ for which this determinant is zero represents the buckling load of the cylinder. This value is found by solving the matrix difference equations by the modified Gaussian elimination method which was described in the prebuckling solution. That is, the first of equations (37) and equation (40) are solved for Z_{B_0} in terms of Z_{B_1} to give

$$Z_{B_0} = \left[-\bar{A}_0 A_0^{-1} B_0 + \bar{B}_0\right]^{-1}\left[\bar{A}_0 A_0^{-1} C_0 - \bar{C}_0\right] Z_{B_1} \tag{42}$$

The recurrence equation is of the form

$$Z_{B_i} = P_i Z_{B_{i+1}} \qquad (i = 0, 1, \ldots, k) \tag{43}$$

and therefore P_0 can be determined as

$$P_0 = \left[-\bar{A}_0 A_0^{-1} B_0 + \bar{B}_0\right]^{-1}\left[\bar{A}_0 A_0^{-1} C_0 - \bar{C}_0\right] \tag{44}$$

Now substituting $Z_{B_{i-1}} = P_{i-1} Z_{B_i}$ into the general equation (37) provides the result

$$P_i = -\left[A_i P_{i-1} + B_i\right]^{-1} C_i \qquad (i = 1, 2, \ldots, k) \tag{45}$$

where P_0 is given by equation (44). Finally, equations (41) and (43) provide the result

$$\left[\bar{A}_k P_{k-1} P_k + \bar{B}_k P_k + \bar{C}_k\right] Z_{B_{k+1}} = 0 \tag{46}$$

Now if for a value of $\hat{N}_x$ the determinant of the coefficient of $Z_{B_{k+1}}$ in equation (46) is zero, then this zero is a zero of the coefficient matrix and this value of $\hat{N}_x$ represents a possible buckling load of the cylinder. The above solution requires only the inversion of 4×4 matrices for the determination of the buckling load and therefore is well suited for rapid calculation on a digital computer.

The actual solution on the computer is done in the following manner: Initially an n, the number of circumferential waves, and an $\hat{N}_x$ are selected (the initial values for n and $\hat{N}_x$ were taken in most cases to be the values obtained from a classical solution, where w_A is constant). The prebuckling displacement and derivatives at each station are then calculated for the selected $\hat{N}_x$ and the value of the determinant of equation (46) is calculated; $\hat{N}_x$ is then iterated until a zero of the determinant corresponding to the smallest value of $\hat{N}_x$ is determined. Then n is changed and the above procedure is repeated to determine a new $\hat{N}_x$; the lowest value of $\hat{N}_x$ which is determined is then taken to be the buckling load. It should be noted that the presence of spurious singularities in the determinant of equation (46) sometimes make determination of the zero of the determinant difficult. This problem was resolved by employing the procedure described in reference 16.

For all the computations a digital computer was used. Because the maximum order of the matrix was 4, a large number of finite-difference stations could be used without exceeding the storage capacity of the computer. For the calculations, the number of stations was increased until an increase in the number of stations did not affect the buckling load to within a specified accuracy. For the cylinders investigated, it was found

that approximately 200 to 300 stations along the length of the shell were required for proper convergence.

In order to evaluate and compare the effect of discrete rings, the solutions of the prebuckling and buckling equations were obtained for the case in which the rings are assumed to be smeared out. This solution is presented in appendix B. It was also of interest to compare the buckling loads obtained herein with buckling loads obtained when classical prebuckling deformations $(w_A = \text{Constant})$ are assumed. For smeared rings the buckling solutions, with classical prebuckling deformations and simple-support boundary conditions assumed, are presented in reference 3. For discrete rings a Galerkin solution of the classical buckling equations is presented in appendix C.

Buckling Shapes

The shape of the buckling displacement along the length of the cylinder was determined by employing the following procedure. The matrix of the coefficients of $Z_{B_{k+1}}$ in equation (46) is defined in the following notation:

$$\left[\bar{A}_k P_{k-1} P_k + \bar{B} P_k + \bar{C}_k\right] = \begin{bmatrix} a_{11} & a_{12} & a_{13} & a_{14} \\ a_{21} & a_{22} & a_{23} & a_{24} \\ a_{31} & a_{32} & a_{33} & a_{34} \\ a_{41} & a_{42} & a_{43} & a_{44} \end{bmatrix} \tag{47}$$

The solution for each of the four elements of the column vector $Z_{B_{k+1}}$, in the notation of equation (47), can be obtained as

$$U_{k+1} = \begin{vmatrix} a_{12} & a_{13} & a_{14} \\ a_{22} & a_{23} & a_{24} \\ a_{42} & a_{43} & a_{44} \end{vmatrix} \tag{48a}$$

$$V_{k+1} = -\begin{vmatrix} a_{11} & a_{13} & a_{14} \\ a_{21} & a_{23} & a_{24} \\ a_{41} & a_{43} & a_{44} \end{vmatrix} \tag{48b}$$

$$W_{k+1} = \begin{vmatrix} a_{11} & a_{12} & a_{14} \\ a_{21} & a_{22} & a_{24} \\ a_{41} & a_{42} & a_{44} \end{vmatrix} \tag{48c}$$

$$M_{k+1} = -\begin{vmatrix} a_{11} & a_{12} & a_{13} \\ a_{21} & a_{22} & a_{23} \\ a_{41} & a_{42} & a_{43} \end{vmatrix} \tag{48d}$$

Equations (48) determine the relative components of $Z_{B_{k+1}}$ and then the remaining Z_{B_i} are calculated in reverse order by using equation (43). Once the Z_{B_i} have been calculated, the buckling displacements w_B at any station along the cylinder are known in terms of an arbitrary constant. Each buckling displacement is then divided by the absolute value of the maximum displacement to obtain the normalized buckling displacements $\frac{w_B}{|w_{B_{max}}|}$.

RESULTS AND DISCUSSION

Because of the large number of geometric and physical parameters involved in this investigation, it is impractical to present results of a general nature. However, it is of value to present some computed results for large-diameter cylinders in order to study the influence of discrete ring stiffeners, prebuckling deformations, and eccentrically applied axial compressive load resultants (applied axial load and edge moment). Thus, computations of axial compressive buckling loads for boundary conditions of simple support were made for two types of stiffened cylinders appropriate for large-diameter booster interstage structures: ring- and stringer-stiffened isotropic cylinders and ring-stiffened corrugated cylinders. In order to compare theory with the test results of reference 7, computations of compressive buckling loads were also made for clamped integrally stiffened and Z-stiffened isotropic cylinders.

The dimensions of the ring- and stringer-stiffened cylinders and of the ring-stiffened corrugated cylinders are given in figure 2 and the dimensions of the integral stiffened and Z-stiffened cylinders are given in reference 7. For the computations, the material in the cylindrical shell and the material in the stiffeners were taken to be identical, a value of 0.32 was assigned to Poisson's ratio for the stiffened isotropic cylinders, and the expressions given in reference 8 were used to compute the orthotropic

shell constants for the corrugated cylinder. Eccentricity effects of the stiffeners were studied by moving the stiffeners from the internal to the external surface of the shell. The results of these computations are presented in tables I to III and in figures 3 to 11. Details and discussion of the computed results follow.

Ring- and Stringer-Stiffened and Corrugated Cylinders

The ring- and stringer-stiffened cylinders and the corrugated cylinders are susceptible to buckling modes of panel instability or general instability, depending upon the number of rings on the cylinder and the eccentricity of the stiffeners. General instability is defined as the buckling mode in which the rings deform radially and the cylinder wall and rings buckle as a composite wall. Panel instability is defined as the buckling mode in which the rings have little or no radial buckling deformation and the cylinder buckles between rings. When discreteness of rings is accounted for, the mode of instability is determined by inspection of the buckling shape.

For the calculations, simple-support boundary conditions of $N_{x_B} = 0$, $v_B = 0$, $w_B = 0$, and $M_{x_B} = 0$ were assumed. The number of rings on the cylinders was varied, and nondimensional buckling loads $\hat{N}_x/E_x$ or $\hat{N}_x/E\bar{t}$ $\left(\text{where } \bar{t} \text{ is the effective thickness of the isotropic cylinder wall, } \frac{A_s}{d} + t\right)$ were calculated by three separate theories:

(a) Discrete rings, taking into account "exact" prebuckling deformations (eqs. (30) to (34) and eqs. (44) to (46))

(b) Smeared rings, taking into account "exact" prebuckling deformations (eq. (B2) and eqs. (44) to (46) with smeared-ring matrix coefficients of appendix D)

(c) Discrete rings, assuming constant prebuckling deformations (eq. (C7))

The term "exact" prebuckling deformations refers to the deformations due to the loading and end-condition restraints that occur prior to buckling. Considering the prebuckling deformations to be a constant gives a buckling analysis which has a membrane state of stress prior to buckling (as done, for example, in refs. 1 to 5). This type of analysis will be referred to as "classical" buckling theory. Calculations were also made by employing the theory of reference 3 (eq. (15)), which is a classical buckling theory. For these calculations, general instability represents the case where the rings are smeared out, and panel instability is taken to be the buckling load which is obtained by considering a simply supported cylinder whose length is equal to the ring spacing.

The nondimensional buckling loads for ring- and stringer-stiffened isotropic cylinders and for ring-stiffened corrugated cylinders are presented in tables I and II and are shown in figures 3, 4, and 5. The calculated values in the tables are given for the governing mode of buckling, panel or general instability (panel-instability values are denoted

by a footnote). In the figures, the nondimensional buckling load $\hat{N}_x/E\bar{t}$ for ring- and stringer-stiffened cylinders and $\hat{N}_x/E_x$ for corrugated cylinders, is plotted against N, the number of rings on the cylinder. The buckling loads for $N = 0$ correspond to buckling of a cylinder with no rings on it. For the calculations presented in tables I and II and figures 3, 4, and 5, the stiffened cylinders are assumed to have the compressive load applied at the middle surface of the cylindrical shell ($\bar{e} = 0$); therefore, the prebuckling state has a moment boundary condition equivalent to that of the buckling state $\left(M_{x_A} = M_{x_B} = 0\right)$.

The computed results for isotropic cylinders stiffened by internal rings and stringers are presented in figure 3. The curves shown in the figure are results obtained by using the classical theory of reference 3. The symbols denote results obtained from the present solution and the comparative solutions presented in appendices A and B. (A similar convention for curves and symbols is followed in figs. 4 and 5.) In figure 3, the coincidence of the curves and square symbols suggests that, in using classical theory, the differences resulting from treating the rings as smeared or discrete members are negligible. When the triangular symbols are compared with the solid curves, the effects of accounting for exact prebuckling deformations in general-instability solutions for smeared rings appear to be small. However, the large differences between the circular symbols and the curves indicate that when both discreteness and prebuckling deformations are taken into account, as is done in the present theory, the predicted buckling loads are substantially lower than results obtained from classical solutions. Furthermore, although results of the classical solution indicate that a transition from panel to general instability will occur when the cylinder is stiffened by more than three rings, the present solution suggests that panel instability occurs in cylinders with as many as seven rings.

A possible explanation of the large differences between classical buckling loads and mode shapes and those obtained from the present solution is associated with the assumption in the present calculations that the load is applied at the middle surface of the cylindrical shell ($\bar{e} = 0$). In the classical solution of reference 3, load is applied (implicitly) near the stringer-shell centroid. (See the discussion in the appendix of ref. 4.) Substantial effects of loading eccentricity (i.e., the effect of varying $\bar{e}$) have been noted in reference 6 for longitudinally stiffened cylinders, and the present results suggest that these effects persist in certain ring- and stringer-stiffened cylinders.

For isotropic cylinders stiffened by external rings and stringers, figure 4 again indicates substantial differences between results obtained from classical solutions and results based on the present theory. As in the case of the internally stiffened cylinders, classical solutions with smeared rings and with discrete rings give virtually identical loads. The effect of accounting for prebuckling deformations in general-instability solutions for smeared rings is somewhat larger than that noted in figure 3 and is again

believed to reflect the loading eccentricity effects already mentioned. Note that the use of the present theory for cylinders with less than three rings yields panel-instability loads that are actually higher than classical buckling loads. Both theories predict transition between panel instability and general instability at nearly the same ring spacing. The coincidence of the triangular and circular symbols on the figure is a consequence of the expected result that increasing the number of rings diminishes the effects of discreteness.

For the ring-stiffened corrugated cylinders studied, the computed results presented in table II and shown in figure 5 indicate that the effect of "exact" prebuckling deformations on the buckling load is negligible. This result is expected because for an axially compressed cylinder, prebuckling deformations are a function of Poisson's ratio, and for a corrugated cylinder the value of the extensional circumferential Poisson's ratio $\tilde{\mu}_y$ is very small. (See ref. 8.) The results for corrugated cylinders also show negligible effects due to discrete rings.

Stringer-Stiffened Cylinders

The influence of $\bar{e}$, the eccentricity of the applied axial compressive load, on the buckling load is presented in table III and is shown in figure 6 for an isotropic cylinder stiffened by internal and external stringers (dimensions given in fig. 2(b)). For the calculations, simple-support boundary conditions $N_{x_B} = 0$, $v_B = 0$, $w_B = 0$, $M_{x_B} = 0$, $w_A = 0$, and $M_{x_A} + \hat{N}_x\bar{e} = 0$ were assumed. In figure 6 the nondimensional buckling load $\hat{N}_x/E\bar{t}$ is plotted against the nondimensional distance $\bar{e}/h$, where $\bar{e}$ is the radial distance from the cylinder's middle surface to a circumferential line on which the applied load $\hat{N}_x$ acts and h is one-half the height of the stringer. (See fig. 2.) An eccentrically applied compressive load is equivalent to an axial compressive load applied at the middle surface of the cylinder plus an axisymmetric end moment. The results presented in table III and figure 6 show that the buckling loads for these cylinders are quite sensitive to the radial position at which the load is applied to the ends of the cylinder. Note that the maximum buckling loads of the configurations investigated can be as much as six times as great as loads obtained by considering alternate loading positions. This increase or decrease in load is an interesting phenomenon for it suggests that the design of end fittings may have an important influence on the strength of stiffened cylindrical structures such as launch-vehicle interstages. This effect, of course, does not occur with clamped cylinders.

In figures 7 and 8, the experimental and theoretical buckling loads are shown for the integrally stiffened and Z-stiffened test cylinders of reference 7. In these figures, the nondimensional compressive buckling load $\hat{N}_x/E\bar{t}$ has been plotted against the length-radius ratio a/R. Calculated curves are shown for the four sets of clamped

boundary conditions given by equations (39), for internally and externally stiffened cylinders. These curves were computed by employing the solutions given by equations (30) to (34) and equations (44) to (46), where, for the selected clamped boundary conditions, the proper terms of the selection matrix $\bar{\alpha}$ are chosen (see appendix D). Also shown for comparison are the curves for the clamped solution of reference 7, which is a classical buckling theory. The computed results in figures 7 and 8 show for the externally stiffened cylinder substantial changes in the buckling load due to taking into account "exact" prebuckling deformations. (Compare the classical-theory curves with the solid curves.) Substantial changes also occur as a result of considering different in-plane boundary conditions. (Compare the solid curve with the dashed curves.) For the internally stiffened cylinder, there are only slight changes in the buckling load due to these effects. The agreement between theoretical and test results shown in figures 7 and 8 is generally good, and it is better when prebuckling deformations are considered than when they are neglected.

Prebuckling and Buckling Shapes

In figures 9 to 11, representative axial prebuckling and buckling shapes are shown for the simply supported stiffened isotropic cylinders previously presented in figures 3, 4, and 6. In figures 9 to 11, the "exact" nondimensional prebuckling deformation w_A/t or the normalized buckling deformation $w_B/|w_{B_{max}}|$ is plotted against the cylinder length x/a.

In figure 9, prebuckling and buckling shapes are shown for cylinders stiffened by external rings and stringers and by internal rings and stringers (all with four rings). Buckling results for these cylinders were presented in figures 3 and 4. The prebuckling shapes shown in figures 9(a) and 9(c) are quite different from the usual prebuckling shape of Föppl found in unstiffened cylinders (ref. 17). The buckling shapes illustrating general-instability and panel-instability modes of buckling, respectively, are shown in figures 9(b) and 9(d).

Prebuckling and buckling shapes for the longitudinally stiffened cylinders of figure 6 are shown in figures 10 and 11. The curves in figure 10 indicate that prebuckling shapes are sensitive to changes in the loading eccentricity parameter $\bar{e}/h$ and that large differences in prebuckling shapes exist between internally and externally stiffened cylinders with similar values of $\bar{e}/h$. These results are reflected in the buckling loads presented in figure 6.

CONCLUDING REMARKS

An analytical investigation has been presented of the buckling of eccentrically stiffened orthotropic cylinders, with discretely located ring stiffeners and "exact" prebuckling deformations included in the analysis. Nonlinear prebuckling equations and boundary conditions and linear buckling equations and boundary conditions have been derived by using energy principles, and solutions for simple-support and clamped boundary conditions have been obtained by the method of finite differences for cylinders loaded with any combination of axial compression and lateral pressure. Solutions were also obtained for "smeared" rings, and a Galerkin solution was obtained for the classical buckling problem (simple membrane prebuckling state) of a simply supported cylinder with discrete rings.

Results of sample calculations have been shown for two types of axially compressed, simple supported, large-diameter, stiffened cylinders in order to illustrate the influence on the buckling load of prebuckling deformations, discrete rings, and eccentricity of applied axial compressive loads. In addition, the buckling loads of clamped longitudinally stiffened cylinders are presented in order to compare the present solutions with available test results.

The calculations presented, which take into account "exact" prebuckling deformations, indicate the following:

1. The buckling load may be either substantially greater or less than that predicted by classical theory.

2. The transition between panel- and general-instability modes of buckling is different from that predicted by classical theory.

3. The buckling load may be decreased for cylinders with few rings by considering the rings to be discretely located; thus, the common practice of "smearing" rings in design analysis can be unconservative.

4. The buckling load may be substantially increased (as much as six times for the cylinders studied) or decreased, depending upon the radial position from the cylinder's middle surface at which the axial compressive load is applied at the ends of the cylinder; thus, the end-fitting design may have an important influence on the strength of stiffened-cylinder structures such as launch-vehicle interstages.

5. However, the results for the ring-stiffened corrugated cylinders confirm the conclusion that effects due to considering prebuckling deformations and discrete rings in corrugated cylinders are negligible.

6. The agreement between test results and theory is better than that previously achieved with theories that do not take into account prebuckling deformations.

The calculations show the sensitivity of stiffened cylinders to the investigated effects and, thus, demonstrate the need for calculations which accurately account for details of shell geometry and loading when investigating the stability of stiffened shell structures.

Langley Research Center,
National Aeronautics and Space Administration,
Langley Station, Hampton, Va., March 13, 1967,
124-08-06-26-23.

APPENDIX A

DERIVATION OF GOVERNING EQUATIONS

In this section the nonlinear equilibrium equations and boundary conditions for an eccentrically stiffened perfect orthotropic cylinder are derived by obtaining strain-energy expressions for the shell, stiffeners, and loadings and by applying the method of minimum potential energy.

Strain-Displacement Relations

For the coordinate system shown in figure 1, the Donnell type nonlinear strain-displacement relationships can be written as

$$\left.\begin{aligned} \epsilon_{x_T} &= \epsilon_x - zw_{,xx} \\ \epsilon_{y_T} &= \epsilon_y - zw_{,yy} \\ \gamma_{xy_T} &= \gamma_{xy} - 2zw_{,xy} \end{aligned}\right\} \tag{A1}$$

where

$$\left.\begin{aligned} \epsilon_x &= u_{,x} + \frac{1}{2}w_{,x}^2 \\ \epsilon_y &= v_{,y} + \frac{w}{R} + \frac{1}{2}w_{,y}^2 \\ \gamma_{xy} &= u_{,y} + v_{,x} + w_{,x}w_{,y} \end{aligned}\right\} \tag{A2}$$

The quantities u, v, and w are the displacements of the middle surface of the orthotropic cylinder wall and a comma denotes partial differentiation with respect to the subscript.

The stiffeners are assumed to behave as beam elements, and thus the stiffener strain-displacement relations can be written as

$$\left.\begin{aligned} \epsilon_{y_r} &= \epsilon_y - zw_{,yy} \\ \epsilon_{x_s} &= \epsilon_x - zw_{,xx} \end{aligned}\right\} \tag{A3}$$

where the subscripts r and s denote rings and stringers, respectively. Equations (A3) specify that the displacements are such that the strain varies linearly across

the depth of the stiffener and satisfies compatibility of the displacements between the stiffener and the surface of the shell to which it is fastened.

Energy of Stiffened Cylinder

Orthotropic shell.- The strain energy of the orthotropic shell Π_c can be expressed in terms of resultant middle-surface forces and moments as

$$\Pi_c = \frac{1}{2}\int_0^{2\pi R}\int_0^{a}\left(\bar{N}_x\epsilon_x + \bar{N}_{xy}\gamma_{xy} + \bar{N}_y\epsilon_y - \bar{M}_x w_{,xx} + 2\bar{M}_{xy}w_{,xy} - \bar{M}_y w_{,yy}\right)dx\,dy \tag{A4}$$

where (see ref. 14)

$$\left.\begin{aligned}
\bar{N}_x &= \frac{E_x}{1 - \tilde{\mu}_x\tilde{\mu}_y}\left(\epsilon_x + \tilde{\mu}_y\epsilon_y\right)\\
\bar{N}_y &= \frac{E_y}{1 - \tilde{\mu}_x\tilde{\mu}_y}\left(\epsilon_y + \tilde{\mu}_x\epsilon_x\right)\\
\bar{N}_{xy} &= G_{xy}\gamma_{xy}\\
\bar{M}_x &= -\frac{D_x}{1 - \mu_x\mu_y}\left(w_{,xx} + \mu_y w_{,yy}\right)\\
\bar{M}_y &= -\frac{D_y}{1 - \mu_x\mu_y}\left(w_{,yy} + \mu_x w_{,xx}\right)\\
\bar{M}_{xy} &= D_{xy}w_{,xy}
\end{aligned}\right\} \tag{A5}$$

and ϵ_x, ϵ_y, and γ_{xy} are given by equations (A2).

Rings.- If the rings are considered to be equally spaced and discretely located along the length of the cylinder, the strain energy Π_r of N rings can be expressed as

$$\Pi_r = \frac{1}{2}\sum_{j=1}^{N}\int_0^{2\pi R}\left(\int_{A_r} E_r\epsilon_{y_r}{}^2 dA_r + G_rJ_r w_{,xy}{}^2\right)_{x=j\ell} dy \tag{A6}$$

where dA_r is an element of the cross-sectional area of the ring A_r, G_rJ_r is its twisting stiffness, and ℓ is the ring spacing. In equation (A6) it is assumed the total circumferential arc length of the ring is approximately the same as that of the middle surface of the shell.

APPENDIX A

In the energy expression, the first term is the expression for the energy associated with bending and extension of a beam and the second term is inserted as an approximation to the energy due to twisting of the ring. The approximation for energy due to twisting results from assuming that the ring twists in such a fashion that its angle of twist is equal to the angle of twist of the shell.

When the ring strain-displacement relation (eqs. (A3)) is substituted into equation (A6) and the integrations are performed over the ring area, the strain energy for N rings becomes

$$\Pi_r = \frac{1}{2}\sum_{j=1}^{N}\int_0^{2\pi R}\int_0^{a}\Big(E_rA_r\epsilon_y^2 - 2E_rA_r\bar{z_r}w_{,yy}\epsilon_y + E_rI_{o_r}w_{,yy}^2 + G_rJ_rw_{,xy}^2\Big)\delta(x-j\ell)\,dx\,dy \tag{A7}$$

where $\bar{z_r}$ is the distance from the centroid of the ring to the middle surface of the shell, I_{o_r} is the moment of inertia of a ring about the middle surface of the shell, and $\delta(x-j\ell)$ is a Dirac delta function defined so that

$$\left.\begin{aligned}\int_{-\infty}^{+\infty} f(x)\,\delta(x-j\ell)\,dx &= f(j\ell) \qquad (x = j\ell)\\ \delta(x-j\ell) &= 0 \qquad (x \neq j\ell)\end{aligned}\right\} \tag{A8}$$

Stringers.- If the stringers are assumed to be closely spaced so that their elastic properties can be averaged over the stringer spacing, the strain energy of the stringers Π_s can be taken as

$$\Pi_s = \frac{1}{2}\int_0^{2\pi R}\int_0^{a}\left(\frac{E_sA_s}{d}\epsilon_x^2 - \frac{2E_sA_s\bar{z}_s}{d}\epsilon_x w_{,xx} + \frac{E_sI_{o_s}}{d}w_{,xx}^2 + \frac{G_sJ_s}{d}w_{,xy}^2\right)dx\,dy \tag{A9}$$

where d is the stringer spacing and the subscript s is used to denote stringer properties.

Applied loads.- The potential energy Π_L associated with applied loads of constant pressure p (positive for external pressure) and an externally applied load resultant $\hat{N}_x$ (positive in compression) is

$$\Pi_L = \int_0^{2\pi R}\int_0^{a} pw\,dx\,dy + \int_0^{2\pi R}\hat{N}_x\left(u - \bar{e}w_{,x}\right)\Big|_0^{a}dy \tag{A10}$$

where $\bar{e}$ is the distance from the middle surface of the orthotropic shell to the line on which the load resultant $\hat{N}_x$ acts. The distance $\bar{e}$ is introduced so that loadings of applied edge moments and axial loads may be represented by a statically equivalent force system.

The total potential energy of the stiffened cylinder Π is the sum of the energies given by equations (A4), (A7), (A9), and (A10):

$$\Pi = \Pi_c + \Pi_r + \Pi_s + \Pi_L \tag{A11}$$

Equilibrium Equations and Boundary Conditions

The nonlinear equilibrium equations and boundary conditions are obtained from equation (A11) by applying the principle of minimum potential energy, which requires the vanishing of the first variation ($\delta\Pi = 0$). After integration by parts and proper regrouping, the nonlinear equilibrium equations for an eccentrically stiffened orthotropic cylinder with discrete rings obtained in the above manner are

$$\left.\begin{aligned} &N_{x,x} + N_{xy,y} = 0 \\ &N_{y,y} + N_{xy,x} = 0 \\ &-M_{x,xx} + M_{xy,xy} - M_{y,yy} + \frac{N_y}{R} - N_x w_{,xx} - N_y w_{,yy} - 2N_{xy} w_{,xy} + p = 0 \end{aligned}\right\} \tag{A12}$$

with the following boundary conditions to be satisfied at each end of the cylinder:

$$\left.\begin{aligned} &N_x + \hat{N}_x = 0 && \text{or} \quad u = 0 \\ &N_{xy} = 0 && \text{or} \quad v = 0 \\ &M_x + \hat{N}_x \bar{e} = 0 && \text{or} \quad w_{,x} = 0 \\ &M_{x,x} - M_{xy,y} + N_x w_{,x} + N_{xy} w_{,y} = 0 && \text{or} \quad w = 0 \end{aligned}\right\} \tag{A13}$$

The stress and moment resultants in equations (A12) and (A13) are

$$N_x = \frac{E_x}{1 - \tilde{\mu}_x \tilde{\mu}_y}\left[u_{,x} + \frac{1}{2} w_{,x}^2 + \tilde{\mu}_y\left(v_{,y} + \frac{w}{R} + \frac{1}{2} w_{,y}^2\right)\right] + \frac{E_s A_s}{d}\left(u_{,x} + \frac{1}{2} w_{,x}^2 - \bar{z}_s w_{,xx}\right) \tag{A14a}$$

$$N_y = \frac{E_y}{1 - \tilde{\mu}_x\tilde{\mu}_y}\left[v,_y + \frac{w}{R} + \frac{1}{2}w,_y{}^2 + \tilde{\mu}_x\left(u,_x + \frac{1}{2}w,_x{}^2\right)\right]$$

$$+ \sum_{j=1}^{N} \delta(x-j\ell)E_rA_r\left(v,_y + \frac{w}{R} + \frac{1}{2}w,_y{}^2 - \bar{z}_rw,_{yy}\right) \tag{A14b}$$

$$N_{xy} = G_{xy}\left(u,_y + v,_x + w,_xw,_y\right) \tag{A14c}$$

$$M_x = -\left[\frac{D_x}{1 - \mu_x\mu_y}\left(w,_{xx} + \mu_yw,_{yy}\right) + \frac{E_sI_{o_s}}{d}w,_{xx} - \frac{E_sA_s\bar{z}_s}{d}\left(u,_x + \frac{1}{2}w,_x{}^2\right)\right] \tag{A14d}$$

$$M_y = -\left\{\frac{D_y}{1 - \mu_x\mu_y}\left(w,_{yy} + \mu_xw,_{xx}\right) + \sum_{j=1}^{N} \delta(x-j\ell)\left[E_rI_{o_r}w,_{yy} - E_rA_r\bar{z}_r\left(v,_y + \frac{w}{R} + \frac{1}{2}w,_y{}^2\right)\right]\right\}$$

(A14e)

$$M_{xy} = \left[2D_{xy} + \frac{G_sJ_s}{d} + \sum_{j=1}^{N} \delta(x-j\ell)G_rJ_r\right]w,_{xy} \tag{A14f}$$

Equations (A12) and (A13) appear in the body of the paper as equations (1) and (2).

APPENDIX B

SOLUTION OF PREBUCKLING AND BUCKLING EQUATIONS FOR SMEARED-OUT RINGS

Prebuckling Solution

It is of interest to present the solution of the prebuckling equation for the case in which the rings are assumed to be smeared out over the ring spacing in order to compare it with the discrete-ring case. When the rings are smeared out, the discrete-ring prebuckling governing equation (8) becomes the following constant-coefficient differential equation:

$$\beta_1 w_A'''' + \beta_2 w_A'' + \left(\beta_3 + \frac{\beta_4}{l}\right) w_A - \beta_5 = 0 \tag{B1}$$

where l is the ring spacing and β_1 to β_5 are defined by equations (9). Equation (B1) has the following analytical solution that satisfies boundary conditions (10):

$$w_A = \gamma_1 \sin \alpha_1 x \sinh \alpha_2 x + \gamma_2 \sin \alpha_1 x \cosh \alpha_2 x + \gamma_3 \cos \alpha_1 x \cosh \alpha_2 x + \gamma_4 \cos \alpha_1 x \sinh \alpha_2 x + \frac{\beta_5}{\beta_3 + \frac{\beta_4}{l}} \tag{B2}$$

where

$$\left.\begin{aligned} \alpha_1 &= \sqrt{\frac{\kappa^2}{2} + \frac{\beta_2}{4\beta_1}} & \kappa^2 &= \sqrt{\frac{\beta_3 + \frac{\beta_4}{l}}{\beta_1}} \\ \alpha_2 &= \sqrt{\frac{\kappa^2}{2} - \frac{\beta_2}{4\beta_1}} & \gamma_3 &= -\frac{\beta_5}{\beta_3 + \frac{\beta_4}{l}} \end{aligned}\right\} \tag{B3}$$

For simply supported shells,

$$\gamma_1 = \frac{\beta_5\left(\alpha_2^2 - \alpha_1^2\right)}{2\alpha_1\alpha_2\left(\beta_3 + \frac{\beta_4}{l}\right)} + \frac{\beta_6}{2\alpha_1\alpha_2\beta_1} \tag{B4a}$$

$$\gamma_2 = \frac{(\cos \alpha_1 a - \cosh \alpha_2 a)\left\{\sinh \alpha_2 a\left[\frac{\beta_6}{\beta_1} + \frac{\beta_5(\alpha_2^2 - \alpha_1^2)}{\beta_3 + \frac{\beta_4}{l}}\right] + \frac{2\alpha_1\alpha_2\beta_5 \sin \alpha_1 a}{\beta_3 + \frac{\beta_4}{l}}\right\}}{2\alpha_1\alpha_2\left[(\cos \alpha_1 a \sinh \alpha_2 a)^2 + (\sin \alpha_1 a \cosh \alpha_2 a)^2\right]} \tag{B4b}$$

$$\gamma_4 = \frac{(\cos \alpha_1 a - \cosh \alpha_2 a)\left\{\sin \alpha_1 a\left[\frac{\beta_6}{\beta_1} + \frac{\beta_5(\alpha_2^2 - \alpha_1^2)}{\beta_3 + \frac{\beta_4}{l}}\right] - \frac{2\alpha_1\alpha_2\beta_5 \sinh \alpha_2 a}{\beta_3 + \frac{\beta_4}{l}}\right\}}{2\alpha_1\alpha_2\left[(\cos \alpha_1 a \sinh \alpha_2 a)^2 + (\sin \alpha_1 a \cosh \alpha_2 a)^2\right]} \tag{B4c}$$

For clamped shells,

$$\gamma_1 = \frac{\beta_5}{\beta_3 + \frac{\beta_4}{l}} \frac{(\alpha_2^2 + \alpha_1^2)\sin \alpha_1 a \sinh \alpha_2 a - \alpha_1\alpha_2(\sinh^2 \alpha_2 a + \sin^2 \alpha_1 a)}{\alpha_2^2 \sin^2 \alpha_1 a - \alpha_1^2 \sinh^2 \alpha_2 a} \tag{B5a}$$

$$\gamma_2 = \frac{\beta_5}{\beta_3 + \frac{\beta_4}{l}} \frac{(\cos \alpha_1 a - \cosh \alpha_2 a)(\alpha_2^2 \sin \alpha_1 a - \alpha_2\alpha_1 \sinh \alpha_2 a)}{\alpha_2^2 \sin^2 \alpha_1 a - \alpha_1^2 \sinh^2 \alpha_2 a} \tag{B5b}$$

$$\gamma_4 = \frac{\beta_5}{\beta_3 + \frac{\beta_4}{l}} \frac{(\cos \alpha_1 a - \cosh \alpha_2 a)(\alpha_1^2 \sinh \alpha_2 a - \alpha_1\alpha_2 \sin \alpha_1 a)}{\alpha_2^2 \sin^2 \alpha_1 a - \alpha_1^2 \sinh^2 \alpha_2 a} \tag{B5c}$$

In equations (B4), β_6 is defined by equation (23). Similar types of solutions for prebuckling displacements are reported in references 6, 9, and 10.

Buckling Solution

When the rings are assumed to be smeared out over the ring spacing, the buckling equations (11) and boundary conditions (12) are still applicable except that the stress and moment resultants defined by equations (13) are defined as follows:

$$
\left.
\begin{aligned}
N_{y_B} &= \frac{E_y}{1 - \tilde{\mu}_x\tilde{\mu}_y}\left[v_{B,y} + \frac{w_B}{R} + \tilde{\mu}_x\left(u_{B,x} + w'_A w_{B,x}\right)\right] + \frac{E_r A_r}{l}\left(v_{B,y} + \frac{w_B}{R} - \bar{z}_r w_{B,yy}\right) \\
M_{y_B} &= -\left[\frac{D_y}{1 - \mu_x\mu_y}\left(w_{B,yy} + \mu_x w_{B,xx}\right) + \frac{E_r I_r}{l} w_{B,yy}\right. \\
&\qquad \left. - \frac{E_r A_r \bar{z}_r}{l}\left(v_{B,y} + \frac{w_B}{R} - \bar{z}_r w_{B,yy}\right)\right] \\
M_{xy_B} &= \left(2D_{xy} + \frac{G_s J_s}{d} + \frac{G_r J_r}{l}\right) w_{B,xy}
\end{aligned}
\right\} \qquad \text{(B6)}
$$

and N_{x_B}, M_{x_B}, and N_{xy_B} are as previously defined by equations (13) and l is the ring spacing. Similar equations for stiffened cylinders are presented in reference 4 except that an isotropic shell is used in reference 4 where an orthotropic shell is considered herein. To solve the smeared-ring buckling equations (11) for the boundary conditions considered herein, the finite-difference method is used. The procedure is exactly the same as previously described for the discrete-ring case, and equations (35) to (46) are the same except for the following three changes: the prebuckling displacements and derivatives are given by the analytic solution of equation (B2); the summation and the Dirac delta function $\sum_{j=1}^{N} \delta(x - j\,l)$ are replaced by $1/l$ in the buckling equations (36) (Λ_1 to Λ_{24} are defined the same); and the matrix coefficients A_i, B_i, and C_i of equations (37) are defined in appendix D.

For the numerical computations, a computer program similar to the program for discrete rings is used with the smeared-ring matrix coefficients A_i, B_i, and C_i, and with the prebuckling displacements given by equation (B2). The same procedure of calculating the buckling load $\hat{N}_x$ is used.

APPENDIX C

CLASSICAL BUCKLING SOLUTION FOR DISCRETE RINGS

When the classical prebuckling displacement state is assumed (that is, w_A = Constant), the classical-theory buckling equations for a stiffened orthotropic cylinder with discrete rings can be determined from equations (11) as

$$\left.\begin{aligned} &N_{x_{B,x}} + N_{xy_{B,y}} = 0 \\ &N_{y_{B,y}} + N_{xy_{B,x}} = 0 \\ &-M_{x_{B,xx}} + M_{xy_{B,xy}} - M_{y_{B,yy}} + \frac{N_{y_B}}{R} + \hat{N}_x w_{B,xx} + pRw_{B,yy} = 0 \end{aligned}\right\} \tag{C1}$$

with boundary conditions of

$$\left.\begin{aligned} &N_{x_B} = 0 \quad \text{or} \quad u_B = 0 \\ &N_{xy_B} = 0 \quad \text{or} \quad -v_B = 0 \\ &M_{x_B} = 0 \quad \text{or} \quad w_{B,x} = 0 \\ &M_{x_{B,x}} - M_{xy_{B,y}} - \hat{N}_x w_{B,x} = 0 \quad \text{or} \quad w_B = 0 \end{aligned}\right\} \tag{C2}$$

where

$$N_{x_B} = \frac{E_x}{1 - \tilde{\mu}_x\tilde{\mu}_y}\left[u_{B,x} + \tilde{\mu}_y\left(v_{B,y} + \frac{w_B}{R}\right)\right] + \frac{E_s A_s}{d}\left(u_{B,x} - \bar{z}_s w_{B,xx}\right) \tag{C3a}$$

$$N_{y_B} = \frac{E_y}{1 - \tilde{\mu}_x\tilde{\mu}_y}\left(v_{B,y} + \frac{w_B}{R} + \tilde{\mu}_x u_{B,x}\right) + \sum_{j=1}^{N} \delta(x - j\ell) E_r A_r\left(v_{B,y} + \frac{w_B}{R} - \bar{z}_r w_{B,yy}\right) \tag{C3b}$$

$$N_{xy_B} = G_{xy}\left(u_{B,y} + v_{B,x}\right) \tag{C3c}$$

$$M_{x_B} = -\left[\frac{D_x}{1 - \mu_x\mu_y}\left(w_{B,xx} + \mu_y w_{B,yy}\right) + \frac{E_s I_s}{d} w_{B,xx} - \frac{E_s A_s \bar{z}_s}{d}\left(u_{B,x} - \bar{z}_s w_{B,xx}\right)\right] \tag{C3d}$$

$$M_{y_B} = -\left\{\frac{D_y}{1 - \mu_x\mu_y}\left(w_{B,yy} + \mu_x w_{B,xx}\right) + \sum_{j=1}^{N} \delta(x - j\ell)\left[E_r I_r w_{B,yy} - E_r A_r \bar{z}_r\left(v_{B,y} + \frac{w_B}{R} - \bar{z}_r w_{B,yy}\right)\right]\right\} \tag{C3e}$$

$$M_{xy_B} = \left[2D_{xy} + \frac{G_s I_s}{d} + \sum_{j=1}^{N} \delta(x - j\ell) G_r J_r\right] w_{B,xy} \tag{C3f}$$

and $\hat{N}_x$ is the compressive load, $N_{y_A} = -pR$, and $N_{xy_A} = 0$.

To obtain a solution for the buckling load which satisfies boundary conditions (C2) of classical simple support $\left(v_B = N_{x_B} = M_{x_B} = w_B = 0\right)$, the buckling displacements are taken as

$$\left.\begin{aligned} u_B &= \cos\frac{ny}{R} \sum_{q=1}^{\infty} c_q \cos\frac{q\pi x}{a} \\ v_B &= \sin\frac{ny}{R} \sum_{q=1}^{\infty} b_q \sin\frac{q\pi x}{a} \\ w_B &= \cos\frac{ny}{R} \sum_{q=1}^{\infty} a_q \sin\frac{q\pi x}{a} \end{aligned}\right\} \tag{C4}$$

where n is the number of circumferential waves and the coefficients a_q, b_q, and c_q are to be determined.

Use of the Galerkin method and a procedure similar to that of reference 11 yields the following set of equations for the unknown coefficients a_q, b_q, and c_q:

$$\left.\begin{aligned}
&\int_0^{2\pi R}\int_0^{a} Q_x(u,v,w)\cos\frac{sy}{R}\cos\frac{r\pi x}{a}\,dx\,dy = 0\\
&\int_0^{2\pi R}\int_0^{a} Q_y(u,v,w)\sin\frac{sy}{R}\sin\frac{r\pi x}{a}\,dx\,dy = 0\\
&\int_0^{2\pi R}\int_0^{a} Q_z(u,v,w)\cos\frac{sy}{R}\sin\frac{r\pi x}{a}\,dx\,dy = 0
\end{aligned}\right\} \quad \begin{pmatrix} s = 0, 1, 2, \ldots \\ r = 1, 2, 3, \ldots \end{pmatrix} \qquad (C5)$$

where Q_x, Q_y, and Q_z are the result of substituting the series for the buckling displacements u, v, and w, equations (C4), into the governing equations (C1).

From equations (C5) the resulting system of equations is determined as

$$\left.\begin{aligned}
&-F_1c_r + F_2b_r + F_3a_r = 0\\
&F_2c_r - F_4b_r - \frac{2F_5}{a}\sum_{j=1}^{N}\sin\frac{r\pi j}{N+1}\sum_{q=1}^{\infty} b_q\sin\frac{q\pi j}{N+1}\\
&- F_6a_r - \frac{2F_7}{a}\sum_{j=1}^{N}\sin\frac{r\pi j}{N+1}\sum_{q=1}^{\infty} a_q\sin\frac{q\pi j}{N+1} = 0\\
&F_3c_r - F_6b_r - \frac{2F_7}{a}\sum_{j=1}^{N}\sin\frac{r\pi j}{N+1}\sum_{q=1}^{\infty} b_q\sin\frac{q\pi j}{N+1}\\
&- \left[F_8 - N_x\left(\frac{r\pi}{a}\right)^2 - pR\left(\frac{n}{R}\right)^2\right]a_r\\
&- \frac{2(F_9 + F_{10})}{a}\sum_{j=1}^{N}\sin\frac{r\pi j}{N+1}\sum_{q=1}^{\infty} a_q\sin\frac{q\pi j}{N+1}\\
&- \frac{2F_{11}}{a}\sum_{j=1}^{N}\frac{r\pi}{a}\cos\frac{r\pi j}{N+1}\sum_{q=1}^{\infty} a_q\frac{q\pi}{a}\cos\frac{q\pi j}{N+1} = 0
\end{aligned}\right\} \quad (r = 1, 2, \ldots) \qquad (C6)$$

where F_1 to F_{11} are defined in appendix D. Equations (C6) give the criteria for buckling if the determinant of the coefficients vanishes, that is,

$$\left|A_{rq}\right| = 0$$

APPENDIX C

By combining equations (C6), the following determinant of the coefficients a_r can be obtained:

$$\left|A_{rq}\right| = \left| \left[F_8 + (F_9 + F_{10})\Phi_r + F_{11}\Psi_r + F_3 \frac{F_2(F_6 + F_7\Phi_r) - F_3(F_4 + F_5\Phi_r)}{F_1(F_4 + F_5\Phi_r) - F_2^2} + (F_6 + F_7\Phi_r)\frac{F_3F_2 - F_1(F_6 + F_7\Phi_r)}{F_1(F_4 + F_5\Phi_r) - F_2^2} - \hat{N}_x\left(\frac{r\pi}{a}\right)^2 - pR\left(\frac{n}{R}\right)^2 \right] \delta_{rq} + F_9\Phi_{rq} + F_{11}\Psi_{rq} \right| = 0 \qquad (r = 1, 2, \ldots;\ q = 1, 2, \ldots) \qquad \text{(C7)}$$

where

$$\left.\begin{aligned} \Phi_r &= \frac{2}{a}\sum_{j=1}^{N} \sin^2\frac{r\pi j}{N+1} \\ \Phi_{rq} &= \frac{2}{a}\sum_{j=1}^{N} \sin\frac{r\pi j}{N+1}\sin\frac{q\pi j}{N+1} \\ \Psi_r &= \frac{2}{a}\sum_{j=1}^{N} \left(\frac{r\pi}{a}\right)^2 \cos^2\frac{r\pi j}{N+1} \\ \Psi_{rq} &= \frac{2}{a}\sum_{j=1}^{N} \frac{r\pi}{a}\frac{q\pi}{a}\cos\frac{r\pi j}{N+1}\cos\frac{q\pi j}{N+1} \end{aligned}\right\} \qquad \text{(C8)}$$

Examination of the determinant given by equation (C7) reveals that the terms with r and q odd are not coupled with the terms with r and q even. Thus, the determinant of equation (C7) may be separated into two determinants, one for r and q odd and one for r and q even. The determinant for r and q odd represents a symmetrical w-deformation and the determinant for r and q even represents an antisymmetrical w-deformation. The form of these two determinants is identical to the determinant of equation (C7) except for the mentioned restrictions on r and q. Each determinant given by equation (C7) (r and q odd, or r and q even) is in the form of a standard eigenvalue problem and is solved on a digital computer. When computing the

buckling load, each determinant is minimized numerically for integral values of n, the number of circumferential waves in the buckle pattern, and the buckling load is taken to be the absolute minimum obtained from the r-and-q-odd determinant and the r-and-q-even determinant. The size of the determinants (r) is determined by requiring that the buckling load converge to a desired accuracy. For the calculations presented herein, the size of the determinants was increased until the buckling load between a determinant of a specified order and a determinant of one less order did not vary to within a specified accuracy. For the cylinders considered herein, a maximum of 10 terms was required for convergence of the series given by equations (C4).

APPENDIX D

FORMULAS FOR COEFFICIENTS

The coefficients $\Lambda_1, \Lambda_2, \ldots, \Lambda_{24}$ appearing in equations (36) are as follows:

$$\Lambda_1 = \frac{E_x}{1 - \tilde{\mu}_x\tilde{\mu}_y} + \frac{E_S A_S}{\bar{D}_x d}\left(\frac{D_x}{1 - \mu_x\mu_y} + \frac{E_S I_S}{d}\right)$$

$$\Lambda_2 = G_{xy}\left(\frac{n}{R}\right)^2$$

$$\Lambda_3 = \left(\frac{E_x\tilde{\mu}_y}{1 - \tilde{\mu}_x\tilde{\mu}_y} + G_{xy}\right)\frac{n}{R}$$

$$\Lambda_4 = \frac{E_x\tilde{\mu}_y}{R\left(1 - \tilde{\mu}_x\tilde{\mu}_y\right)} - \frac{D_x\mu_y E_S A_S \bar{z}_S}{\bar{D}_x\left(1 - \mu_x\mu_y\right)d}\left(\frac{n}{R}\right)^2$$

$$\Lambda_5 = \frac{E_S A_S \bar{z}_S}{\bar{D}_x d}$$

$$\Lambda_6 = G_{xy}$$

$$\Lambda_7 = \frac{E_y}{1 - \tilde{\mu}_x\tilde{\mu}_y}\left(\frac{n}{R}\right)^2$$

$$\Lambda_8 = E_r A_r\left(\frac{n}{R}\right)^2$$

$$\Lambda_9 = \frac{E_y n}{R^2\left(1 - \tilde{\mu}_x\tilde{\mu}_y\right)}$$

$$\Lambda_{10} = G_{xy}\frac{n}{R}$$

$$\Lambda_{11} = \frac{E_r A_r n}{R}\left[\frac{1}{R} + \bar{z}_r\left(\frac{n}{R}\right)^2\right]$$

APPENDIX D

$$\Lambda_{12} = \frac{E_y \tilde{\mu}_x}{R\left(1 - \tilde{\mu}_x \tilde{\mu}_y\right)}$$

$$\Lambda_{13} = \frac{E_x}{1 - \tilde{\mu}_x \tilde{\mu}_y} + \frac{E_s A_s}{d}$$

$$\Lambda_{14} = \frac{E_x \tilde{\mu}_y}{1 - \tilde{\mu}_x \tilde{\mu}_y} \frac{n}{R}$$

$$\Lambda_{15} = \left(\frac{D_y \mu_x}{1 - \mu_x \mu_y} + 2D_{xy} + \frac{G_s J_s}{d}\right)\left(\frac{n}{R}\right)^2$$

$$\Lambda_{16} = \frac{E_s A_s \bar{z}_s}{d}$$

$$\Lambda_{17} = G_r J_r \left(\frac{n}{R}\right)^2$$

$$\Lambda_{18} = \frac{D_y}{1 - \mu_x \mu_y}\left(\frac{n}{R}\right)^4 + \frac{E_y}{R^2\left(1 - \tilde{\mu}_x \tilde{\mu}_y\right)}$$

$$\Lambda_{19} = \frac{E_y \tilde{\mu}_x}{\bar{E}_x\left(1 - \tilde{\mu}_x \tilde{\mu}_y\right)}\left(\frac{n}{R}\right)^2$$

$$\Lambda_{20} = \frac{E_y \tilde{\mu}_x E_s A_s \bar{z}_s}{\bar{E}_x\left(1 - \tilde{\mu}_x \tilde{\mu}_y\right) d}\left(\frac{n}{R}\right)^2 - \frac{E_y \tilde{\mu}_x}{R\left(1 - \tilde{\mu}_x \tilde{\mu}_y\right)}$$

$$\Lambda_{21} = \frac{E_y\left(E_x + \frac{E_s A_s}{d}\right)}{\bar{E}_x R\left(1 - \tilde{\mu}_x \tilde{\mu}_y\right)}\left(\frac{n}{R}\right)^2$$

$$\Lambda_{22} = \left(E_r I_r + E_r A_r \bar{z}_r^2\right)\left(\frac{n}{R}\right)^4 + \frac{2E_r A_r \bar{z}_r n^2}{R^3} + \frac{E_r A_r}{R^2}$$

$$\Lambda_{23} = \frac{E_r A_r n^2}{R^3}$$

$$\Lambda_{24} = \frac{D_x \mu_y}{1 - \mu_x \mu_y}\left(\frac{n}{R}\right)^2$$

APPENDIX D

The coefficient matrices A_i, B_i, and C_i appearing in equation (37) are as follows.

For discrete rings:

$$A_i = \begin{bmatrix} \Lambda_1 & -\frac{\Delta\Lambda_3}{2} & \left(w'_A - \frac{\Delta}{2}w''_A\right)\Lambda_1 - \frac{\Delta\Lambda_4}{2} & -\frac{\Delta\Lambda_5}{2} \\ \frac{\Delta\Lambda_3}{2} & \Lambda_6 & \frac{\Delta\Lambda_3 w'_A}{2} & 0 \\ \frac{\Delta}{2}\left(\Lambda_{13}w''_A - \Lambda_{12}\right) & 0 & -\Lambda_{15} + \hat{N}_x + \Lambda_{16}w''_A + \frac{\Delta}{2}\left(\Lambda_{13}w''_A - \Lambda_{12}\right)w'_A \\ & & + \frac{\Lambda_{17}}{\Delta}\left[\frac{\delta_{(i+1)H}}{4} - \delta_{iH} - \frac{\delta_{(i-1)H}}{4}\right] & -1 \\ \frac{\Delta\Lambda_{16}}{2} & 0 & \bar{D}_x + \frac{\Delta\Lambda_{16}}{2}w'_A & 0 \end{bmatrix}$$

$$B_i = \begin{bmatrix} -2\Lambda_1 - \Delta^2\Lambda_2 & 0 & -\left(2\Lambda_1 + \Delta^2\Lambda_2\right)w'_A & 0 \\ 0 & -2\Lambda_6 - \Delta^2\Lambda_7 - \Delta\Lambda_8\delta_{iH} & -\Delta^2\Lambda_9 - \Delta^2\Lambda_{10}w''_A - \Delta\Lambda_{11}\delta_{iH} & 0 \\ 0 & \Delta^2\Lambda_9 - \Delta^2\Lambda_{14}w''_A + \Delta\Lambda_{11}\delta_{iH} & 2\Lambda_{15} + \Delta^2\Lambda_{18} - \left(2 + \Delta^2\Lambda_{19}\right)\hat{N}_x + \left(\Delta^2\Lambda_{20} - 2\Lambda_{16}\right)w''_A + \Delta^2\Lambda_{21}w_A + \left(\frac{2\Lambda_{17}}{\Delta} + \Delta\Lambda_{22} + \Delta\Lambda_{23}w_A\right)\delta_{iH} & 2 \\ 0 & 0 & -2\bar{D}_x - \Delta^2\Lambda_{24} & \Delta^2 \end{bmatrix}$$

APPENDIX D

$$C_i = \begin{bmatrix} \Lambda_1 & \frac{\Delta\Lambda_3}{2} & \left(w'_A + \frac{\Delta}{2}w''_A\right)\Lambda_1 + \frac{\Delta\Lambda_4}{2} & \frac{\Delta\Lambda_5}{2} \\ -\frac{\Delta\Lambda_3}{2} & \Lambda_6 & -\frac{\Delta\Lambda_3 w'_A}{2} & 0 \\ \frac{\Delta}{2}\left(\Lambda_{12} - \Lambda_{13}w''_A\right) & 0 & \begin{array}{l} -\Lambda_{15} + \hat{N}_x + \Lambda_{16}w''_A \\ + \frac{\Delta}{2}\left(\Lambda_{12} - \Lambda_{13}w''_A\right)w'_A \\ + \frac{\Lambda_{17}}{\Delta}\left[\frac{\delta_{(i-1)H}}{4} - \delta_{iH} - \frac{\delta_{(i+1)H}}{4}\right] \end{array} & -1 \\ -\frac{\Delta\Lambda_{16}}{2} & 0 & \bar{D}_x - \frac{\Delta\Lambda_{16}w'_A}{2} & 0 \end{bmatrix}$$

where the subscript H of the Kronecker delta is as defined by equation (19).

For smeared rings:

$$A_i = \begin{bmatrix} \Lambda_1 & -\frac{\Delta\Lambda_3}{2} & \left(w'_A - \frac{\Delta}{2}w''_A\right)\Lambda_1 - \frac{\Delta}{2}\Lambda_4 & -\frac{\Delta\Lambda_5}{2} \\ \frac{\Delta\Lambda_3}{2} & \Lambda_6 & \frac{\Delta\Lambda_3}{2}w'_A & 0 \\ \frac{\Delta}{2}\left(\Lambda_{13}w''_A - \Lambda_{12}\right) & 0 & \begin{array}{l} -\Lambda_{15} + \hat{N}_x + \Lambda_{16}w''_A \\ + \frac{\Delta}{2}\left(\Lambda_{13}w''_A - \Lambda_{12}\right)w'_A - \frac{\Lambda_{17}}{l} \end{array} & -1 \\ \frac{\Delta\Lambda_{16}}{2} & 0 & \bar{D}_x + \frac{\Delta\Lambda_{16}w'_A}{2} & 0 \end{bmatrix}$$

$$B_i = \begin{bmatrix} -2\Lambda_1 - \Delta^2\Lambda_2 & 0 & -\left(2\Lambda_1 + \Delta^2\Lambda_2\right)w'_A & 0 \\ 0 & -2\Lambda_6 - \Delta^2\Lambda_7 - \dfrac{\Delta^2\Lambda_8}{l} & -\Delta^2\Lambda_9 - \Delta^2\Lambda_{10}w''_A - \dfrac{\Delta^2\Lambda_{11}}{l} & 0 \\ 0 & \Delta^2\Lambda_9 - \Delta^2\Lambda_{14}w''_A + \dfrac{\Delta^2\Lambda_{11}}{l} & \begin{aligned} &2\Lambda_{15} + \Delta^2\Lambda_{18} - \left(2 + \Delta^2\Lambda_{19}\right)\hat{N}_x \\ &+ \left(\Delta^2\Lambda_{20} - 2\Lambda_{16}\right)w''_A \\ &+ \Delta^2\Lambda_{21}w_A + 2\,\frac{\Lambda_{17}}{l} + \Delta^2\,\frac{\Lambda_{22}}{l} \\ &+ \frac{\Delta^2\Lambda_{23}}{l}\,w_A \end{aligned} & 2 \\ 0 & 0 & -2\bar{D}_x - \Delta^2\Lambda_{24} & \Delta^2 \end{bmatrix}$$

$$C_i = \begin{bmatrix} \Lambda_1 & \dfrac{\Delta\Lambda_3}{2} & \left(w'_A + \dfrac{\Delta}{2}w''_A\right)\Lambda_1 + \dfrac{\Delta\Lambda_4}{2} & \dfrac{\Delta\Lambda_5}{2} \\ -\dfrac{\Delta\Lambda_3}{2} & \Lambda_6 & -\dfrac{\Delta\Lambda_3 w'_A}{2} & 0 \\ \dfrac{\Delta}{2}\left(\Lambda_{12} - \Lambda_{13}w''_A\right) & 0 & \begin{aligned} &-\Lambda_{15} + \hat{N}_x + \Lambda_{16}w''_A \\ &-\frac{\Delta}{2}\left(\Lambda_{13}w''_A - \Lambda_{12}\right)w'_A - \frac{\Lambda_{17}}{l} \end{aligned} & -1 \\ -\dfrac{\Delta\Lambda_{16}}{2} & 0 & \bar{D}_x - \dfrac{\Delta\Lambda_{16}w'_A}{2} & 0 \end{bmatrix}$$

APPENDIX D

The coefficient matrices $\bar{A}_{0(k)}$, $\bar{B}_{0(k)}$, and $\bar{C}_{0(k)}$ appearing in equations (40) and (41) are as follows:

$$\bar{A}_{0(k)} = \bar{\alpha}\begin{bmatrix} -\frac{\Delta\Lambda_{13}}{2} & 0 & -\frac{\Delta\Lambda_{13}}{2}w'_A - \Lambda_{16} & 0 \\ 0 & -\frac{\Lambda_6}{2} & 0 & 0 \\ 0 & 0 & 0 & 0 \\ \frac{\Delta\Lambda_{16}}{2} & 0 & 0 & 0 \end{bmatrix}$$

$$\bar{B}_{0(k)} = \bar{\alpha}\begin{bmatrix} 0 & \Delta^2\Lambda_{14} & \Delta^2\Lambda_{12} + \Lambda_{16} & 0 \\ -\Delta\Lambda_{10} & 0 & -\Delta\Lambda_{10}w'_A & 0 \\ 0 & 0 & 0 & 0 \\ 0 & 0 & -2\bar{D}_x - \Delta^2\Lambda_{24} & \Delta^2 \end{bmatrix} + \begin{bmatrix} 1 - \bar{\alpha}_{11} & 0 & 0 & 0 \\ 0 & 1 - \bar{\alpha}_{22} & 0 & 0 \\ 0 & 0 & 1 & 0 \\ 0 & 0 & 0 & 1 - \bar{\alpha}_{44} \end{bmatrix}$$

$$\bar{C}_{0(k)} = \bar{\alpha}\begin{bmatrix} \frac{\Delta\Lambda_{13}}{2} & 0 & \frac{\Delta\Lambda_{13}}{2}w'_A - \Lambda_{16} & 0 \\ 0 & \frac{\Lambda_6}{2} & 0 & 0 \\ 0 & 0 & 0 & 0 \\ -\frac{\Delta\Lambda_{16}}{2} & 0 & 2\bar{D}_x & 0 \end{bmatrix}$$

where

$$\bar{\alpha} = \begin{bmatrix} \bar{\alpha}_{11} & 0 & 0 & 0 \\ 0 & \bar{\alpha}_{22} & 0 & 0 \\ 0 & 0 & 0 & 0 \\ 0 & 0 & 0 & \bar{\alpha}_{44} \end{bmatrix}$$

APPENDIX D

The elements $\bar{\alpha}_{11}$, $\bar{\alpha}_{22}$, and $\bar{\alpha}_{44}$ of the selection matrix $\bar{\alpha}$ take on the value 1 or 0 depending upon the prescribed boundary conditions. The selection matrix $\bar{\alpha}$ is used to select the prescribed boundary conditions in the following manner: if $\bar{\alpha}_{11}$, $\bar{\alpha}_{22}$, or $\bar{\alpha}_{44}$ equals 1, then $N_{x_B} = 0$, $N_{xy_B} = 0$, or $w_{B,x} = 0$, respectively; and if $\bar{\alpha}_{11}$, $\bar{\alpha}_{22}$, or $\bar{\alpha}_{44}$ equals 0, then $u_B = 0$, $v_B = 0$, or $M_{x_B} = 0$, respectively. For the simple-support boundary conditions considered herein $\left(N_{x_B} = 0,\ v_B = 0,\ M_{x_B} = 0\right)$, $\bar{\alpha}_{11} = 1$, $\bar{\alpha}_{22} = 0$, and $\bar{\alpha}_{44} = 0$, respectively.

The coefficients $F_1, F_2, \ldots, F_{11}$ appearing in equations (C6) are as follows:

$$F_1 = \left(\frac{E_x}{1 - \tilde{\mu}_x\tilde{\mu}_y} + \frac{E_sA_s}{d}\right)\left(\frac{r\pi}{a}\right)^2 + G_{xy}\left(\frac{n}{R}\right)^2$$

$$F_2 = \left(\frac{E_x\tilde{\mu}_y}{1 - \tilde{\mu}_x\tilde{\mu}_y} + G_{xy}\right)\frac{r\pi}{a}\,\frac{n}{R}$$

$$F_3 = \frac{E_x\tilde{\mu}_y}{R\left(1 - \tilde{\mu}_x\tilde{\mu}_y\right)}\,\frac{r\pi}{a} + \frac{E_sA_s\bar{z}_s}{d}\left(\frac{r\pi}{a}\right)^3$$

$$F_4 = \frac{E_y}{1 - \tilde{\mu}_x\tilde{\mu}_y}\left(\frac{n}{R}\right)^2 + G_{xy}\left(\frac{r\pi}{a}\right)^2$$

$$F_5 = E_rA_r\left(\frac{n}{R}\right)^2$$

$$F_6 = \frac{E_yn}{R^2\left(1 - \tilde{\mu}_x\tilde{\mu}_y\right)}$$

$$F_7 = E_rA_r\,\frac{n}{R}\left[\frac{1}{R} + \bar{z}_r\left(\frac{n}{R}\right)^2\right]$$

$$F_8 = \left(\frac{D_x}{1 - \mu_x\mu_y} + \frac{E_sI_s}{d} + \frac{E_sA_s\bar{z}_s^2}{d}\right)\left(\frac{r\pi}{a}\right)^4 + \left(\frac{2D_x\mu_y}{1 - \mu_x\mu_y} + 2D_{xy} + \frac{G_sI_s}{d}\right)\left(\frac{n}{R}\right)^2\left(\frac{r\pi}{a}\right)^2$$
$$+ \frac{D_y}{1 - \mu_x\mu_y}\left(\frac{n}{R}\right)^4 + \frac{E_y}{R^2\left(1 - \tilde{\mu}_x\tilde{\mu}_y\right)}$$

$$F_9 = E_rI_r\left(\frac{n}{R}\right)^4$$

$$F_{10} = E_r A_r \left[\left(\frac{1}{R} \right)^2 + \frac{2\bar{z}_r n^2}{R^3} + \bar{z}_r{}^2 \left(\frac{n}{R} \right)^4 \right]$$

$$F_{11} = G_r J_r \left(\frac{n}{R} \right)^2$$

REFERENCES

1. Van der Neut, A.: The General Instability of Stiffened Cylindrical Shells Under Axial Compression. Rept. S. 314, Nat. Aeron. Res. Inst. (Amsterdam), 1947.

2. Baruch, M.; and Singer, J.: Effect of Eccentricity of Stiffeners on the General Instability of Stiffened Cylindrical Shells Under Hydrostatic Pressure. J. Mech. Eng. Sci., vol. 5, no. 1, 1963, pp. 23-27.

3. Block, David L.; Card, Michael F.; and Mikulas, Martin M., Jr.: Buckling of Eccentrically Stiffened Orthotropic Cylinders. NASA TN D-2960, 1965.

4. McElman, John A.; Mikulas, Martin M., Jr.; and Stein, Manuel: Static and Dynamic Effects of Eccentric Stiffening of Plates and Cylindrical Shells. AIAA J., vol. 4, no. 5, May 1966, pp. 887-894.

5. Hedgepeth, John M.; and Hall, David B.: Stability of Stiffened Cylinders. AIAA J., vol. 3, no. 12, Dec. 1965, pp. 2275-2286.

6. Stuhlman, C.; DeLuzio, A.; and Almroth, B.: Influence of Stiffener Eccentricity and End Moment on Stability of Cylinders in Compression. AIAA J., vol. 4, no. 5, May 1966, pp. 872-877.

7. Card, Michael F.; and Jones, Robert M.: Experimental and Theoretical Results for Buckling of Eccentrically Stiffened Cylinders. NASA TN D-3639, 1966.

8. Peterson, James P.; and Anderson, James Kent: Bending Tests of Large-Diameter Ring-Stiffened Corrugated Cylinders. NASA TN D-3336, 1966.

9. Stein, Manuel: The Influence of Prebuckling Deformations and Stresses on the Buckling of Perfect Cylinders. NASA TR R-190, 1964.

10. Almroth, B. O.: Influence of Edge Conditions on the Stability of Axially Compressed Cylindrical Shells. NASA CR-161, 1965.

11. Block, David L.: Influence of Ring Stiffeners on Instability of Orthotropic Cylinders in Axial Compression. NASA TN D-2482, 1964.

12. Budiansky, Bernard; and Radkowski, Peter P.: Numerical Analysis of Unsymmetrical Bending of Shells of Revolution. AIAA J., vol. 1, no. 8, Aug. 1963, pp. 1833-1842.

13. Cooper, Paul A.: Vibration and Buckling of Prestressed Shells of Revolution. NASA TN D-3831, 1967.

14. Stein, Manuel; and Mayers, J.: A Small-Deflection Theory for Curved Sandwich Plates. NACA Rept. 1008, 1951. (Supersedes NACA TN 2017.)

15. Potters, M. L.: A Matrix Method for the Solution of a Linear Second Order Difference Equation in Two Variables. MR 19, Math. Centrum (Amsterdam), 1955. (Reviewed by J. M. Hedgepeth in Appl. Mech. Rev., vol. 9, no. 3, Mar. 1956, p. 93.)

16. Blum, Robert E.; and Fulton, Robert E.: A Modification of Potter's Method for Solving Eigenvalue Problems Involving Tridiagonal Matrices. AIAA J., vol. 4, no. 12, Dec. 1966, pp. 2231-2232.

17. Föppl, L.: Achsensymmetrisches Ausknicken Zylindrischer Schalen. S.-B. Bayr. Akad. Wiss., 1926, pp. 27-40.

TABLE I.- BUCKLING CALCULATIONS FOR SIMPLY SUPPORTED AXIALLY COMPRESSED RING- AND STRINGER-STIFFENED ISOTROPIC CYLINDERS

Number of rings	Discrete rings, "exact" prebuckling deformations		Smeared rings, "exact" prebuckling deformations		Discrete rings, "classical" theory		"Classical" theory of reference 3	
N	$\hat{N}_x/E\bar{t}$	n	$\hat{N}_x/E\bar{t}$	n	$\hat{N}_x/E\bar{t}$	n	$\hat{N}_x/E\bar{t}$	n
Rings external; stringers external								
0	0.00085	16	0.00085	16	0.00058	19	0.00058	19
1	[a].00238	18	.00314	6	[a].00134	25	[a].00134	25
2	[a].00284	19	.00323	7	[a].00241	26	[a].00241	26
3	.00320	7	.00351	7	[a].00361	18	[a].00361	18
4	.00353	6	.00368	6	.00447	7	.00447	7
5	.00376	6	.00382	6	.00463	7	.00463	7
6	.00391	6	.00395	6	.00478	7	.00478	7
7	.00403	6	.00415	5	.00493	5	.00493	5
Rings internal; stringers internal								
0	0.00017	16	0.00017	16	0.00022	15	0.00022	15
1	[a].00041	27	.00211	9	[a].00064	17	[a].00064	17
2	[a].00068	62	.00242	8	[a].00139	18	[a].00139	18
3	[a].00095	89	.00262	8	[a].00244	19	[a].00244	19
4	[a].00129	112	.00281	8	.00299	7	.00299	7
5	[a].00162	138	.00293	8	.00309	7	.00309	7
6	[a].00214	162	.00297	8	.00320	7	.00320	7
7	[a].00263	183	.00304	8	.00329	8	.00329	8

[a]Buckling in panel-instability mode.

TABLE II.- BUCKLING CALCULATIONS FOR SIMPLY SUPPORTED AXIALLY COMPRESSED RING-STIFFENED CORRUGATED CYLINDERS

Number of rings	Discrete rings, "exact" prebuckling deformations		Smeared rings, "exact" prebuckling deformations		Discrete rings, "classical" theory		"Classical" theory of reference 3	
N	$\hat{N}_x/E_x$	n	$\hat{N}_x/E_x$	n	$\hat{N}_x/E_x$	n	$\hat{N}_x/E_x$	n
Rings internal								
0	0.00050	0	0.00050	0	0.00050	0	0.00050	0
1	.00096	6	.00098	6	.00097	6	.00098	6
2	.00115	6	.00116	6	.00116	6	.00116	6
3	.00133	6	.00133	6	.00133	6	.00133	6
4	.00149	6	.00150	6	.00150	6	.00150	6
5	.00166	6	.00166	6	.00166	6	.00166	6
6	.00182	6	.00182	6	.00182	6	.00182	6
7	.00198	6	.00198	6	.00198	6	.00198	6
Rings external								
0	0.00050	0	0.00050	0	0.00050	0	0.00050	0
1	[a].00197	0	.00290	0	[a].00197	0	[a].00198	0
2	.00326	0	.00337	0	.00336	0	.00337	0
3	.00380	0	.00383	0	.00383	0	.00383	0
4	.00428	0	.00429	0	.00429	0	.00429	0
5	.00474	0	.00475	0	.00475	0	.00475	0
6	.00520	0	.00521	0	.00522	0	.00522	0
7	.00567	0	.00567	0	.00568	0	.00568	0

[a]Buckling in panel-instability mode.

TABLE III.- INFLUENCE OF ECCENTRICALLY APPLIED COMPRESSIVE LOADS ON BUCKLING LOADS OF SIMPLY SUPPORTED STRINGER-STIFFENED ISOTROPIC CYLINDERS

$\bar{e}/h$	$\hat{N}_x/E\bar{t}$	n
	Stringers internal	
1.0	0.000111	17
0	.000171	16
-1.0	.000298	14
-2.0	.000489	13
-3.0	.000618	13
-4.0	.000649	16
-5.0	.000630	16
-6.0	.000599	17
	Stringers external	
2.0	0.000220	26
1.5	.000312	24
1.0	.000494	20
.5	.000740	17
0	.000851	16
-.5	.000841	19
-1.0	.000724	32
-1.5	.000628	36
-2.0	.000557	41

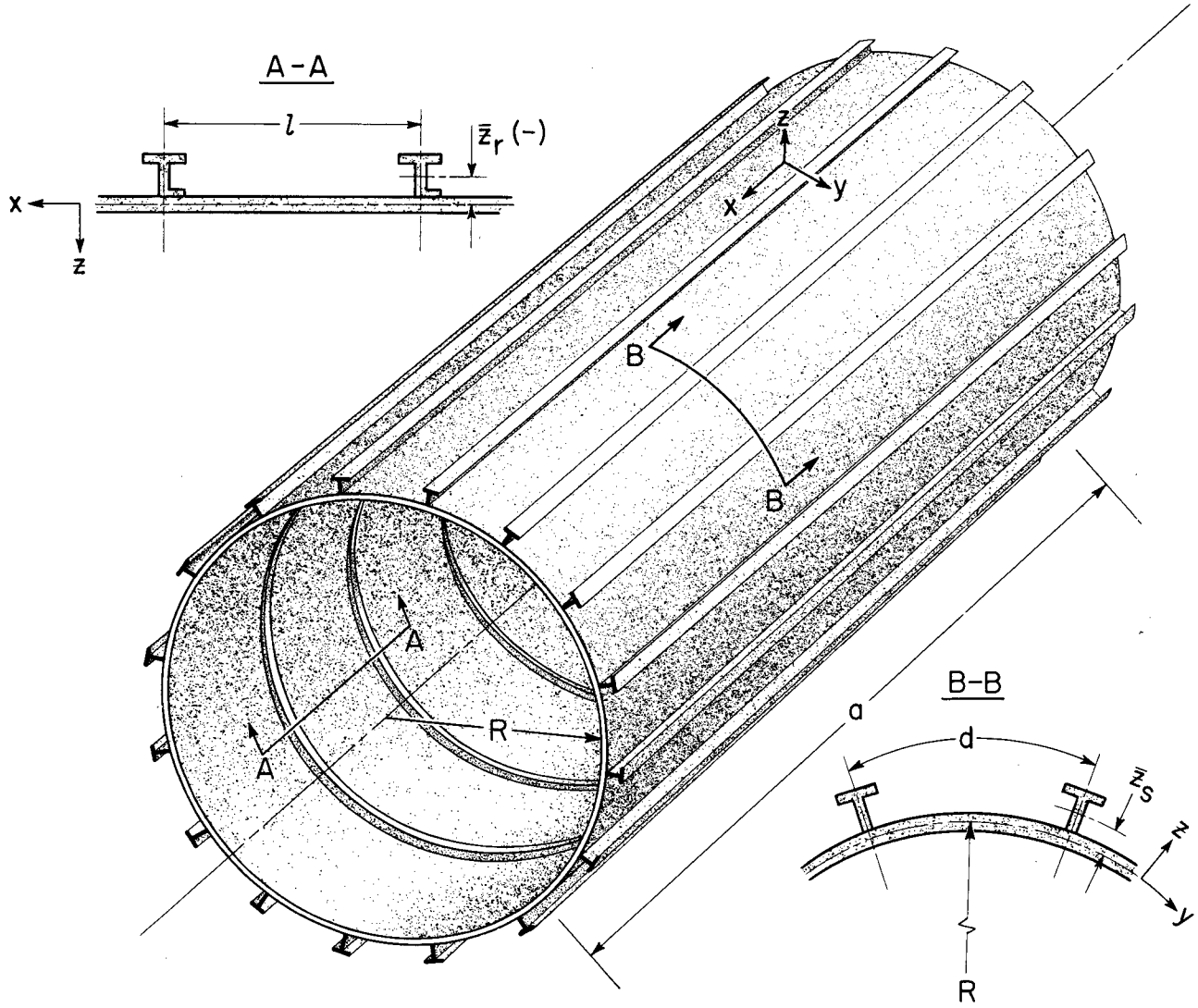

Figure 1.- Geometry of eccentrically stiffened cylinder.

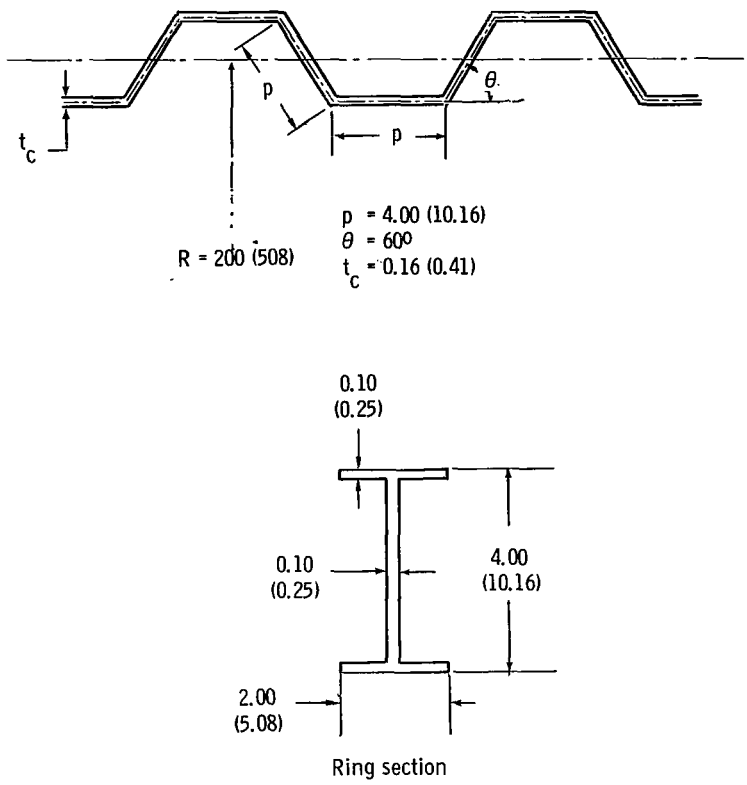

(a) Ring-stiffened corrugated cylinders. a = 200 in. (508 cm).

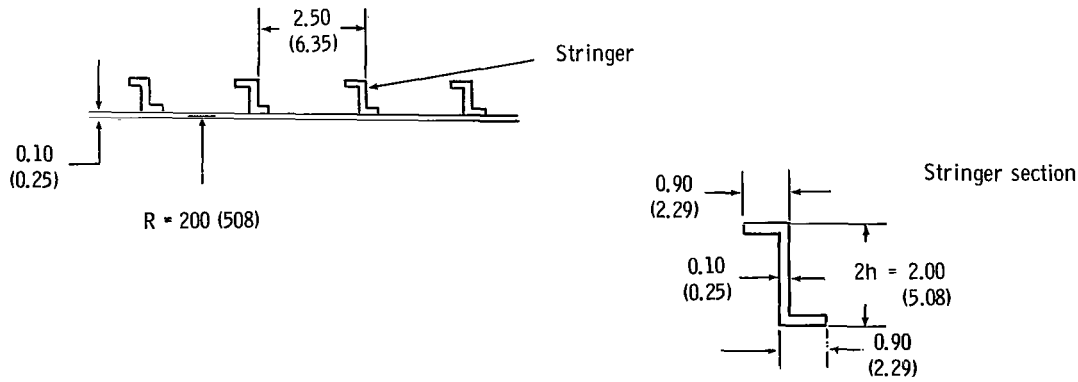

(b) Ring- and stringer-stiffened isotropic cylinder.
a = 200 in. (508 cm). (See fig. 2(a) for ring section.)

Figure 2.- Dimensions of stiffened cylinder. Dimensions are in inches.
(Parenthetical dimensions in cm.)

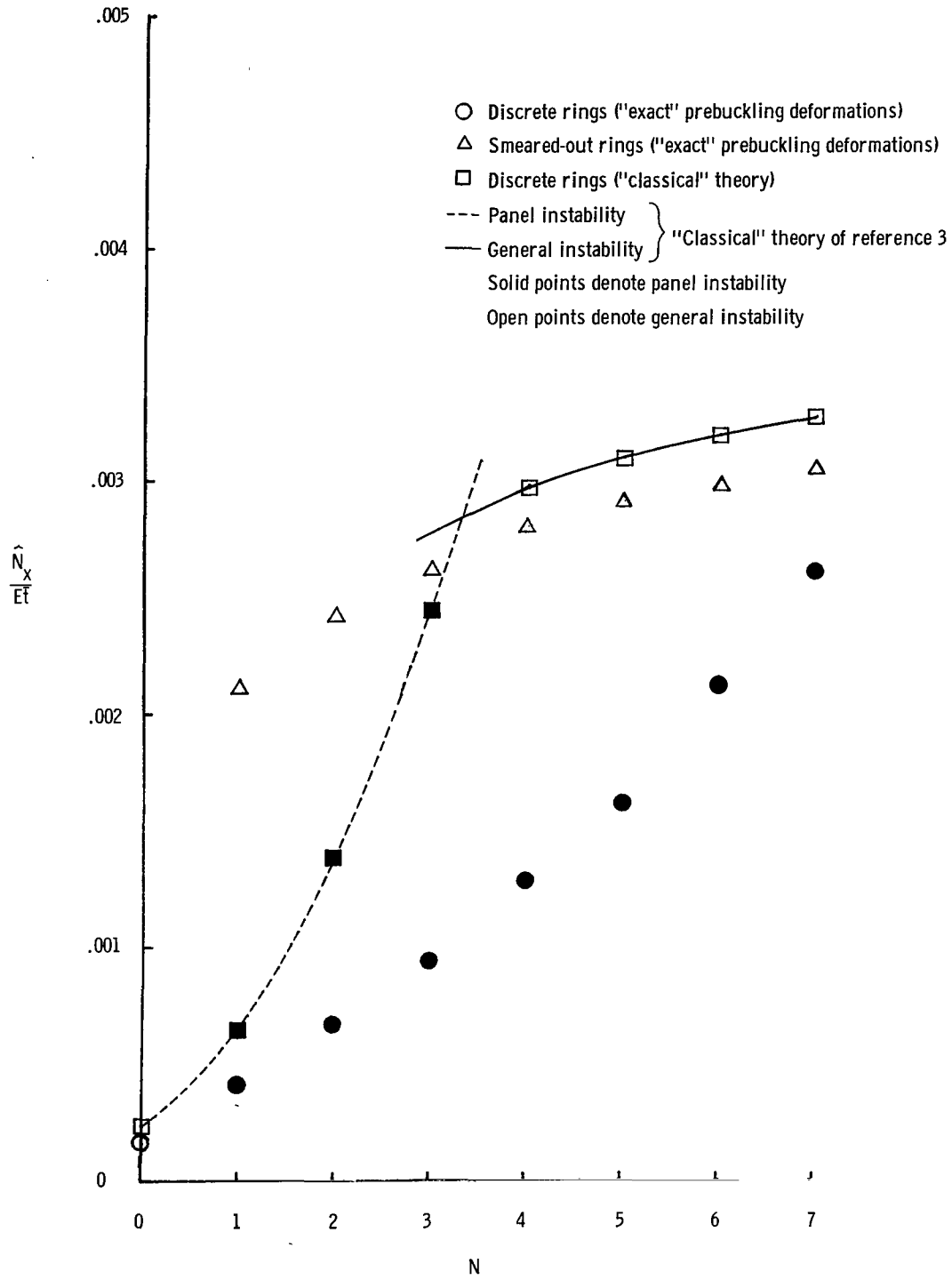

Figure 3.- Buckling predictions for simply supported axially compressed isotropic cylinders stiffened by internal rings and internal stringers.

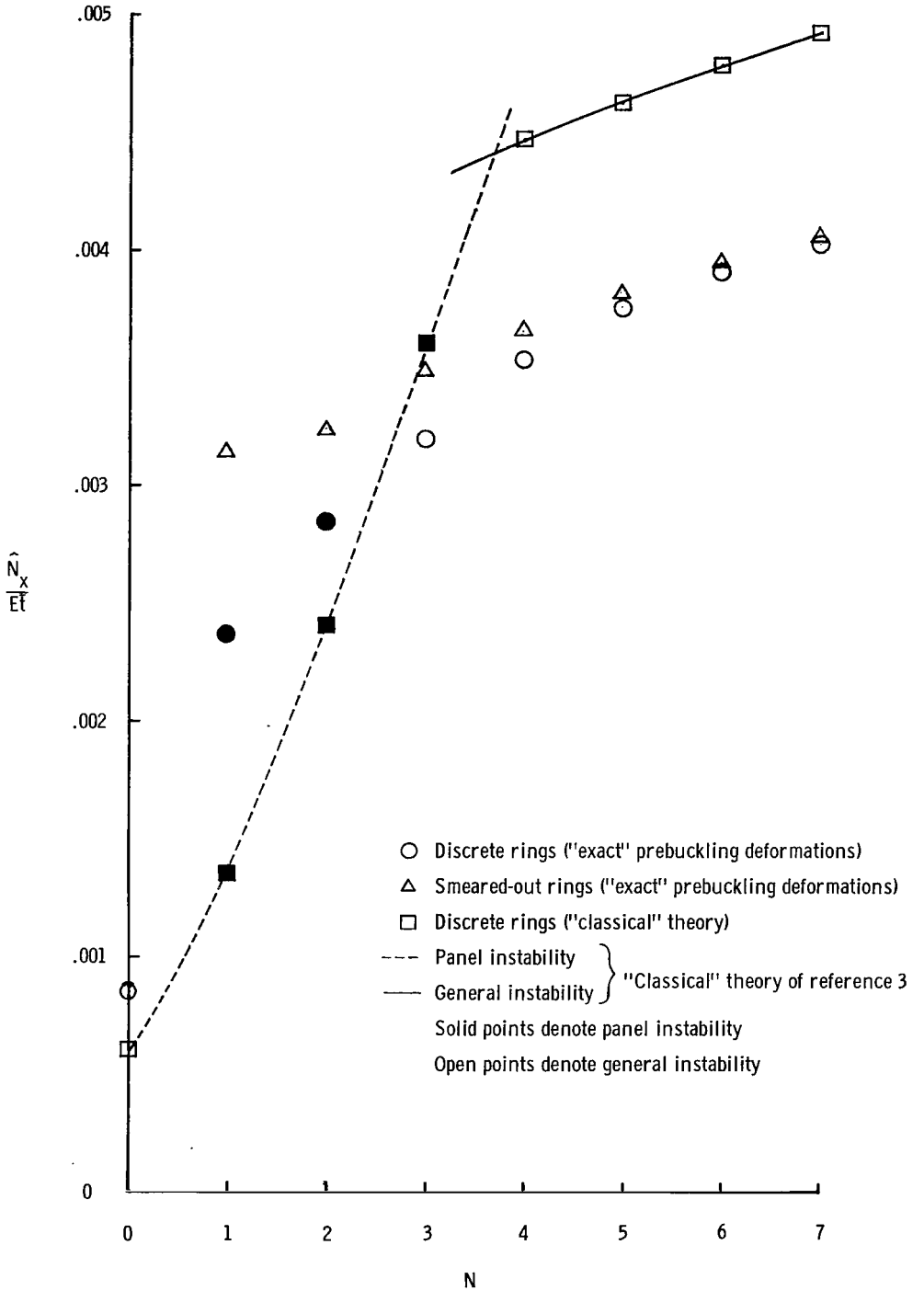

Figure 4.- Buckling predictions for simply supported axially compressed isotropic cylinders stiffened by external rings and external stringers.

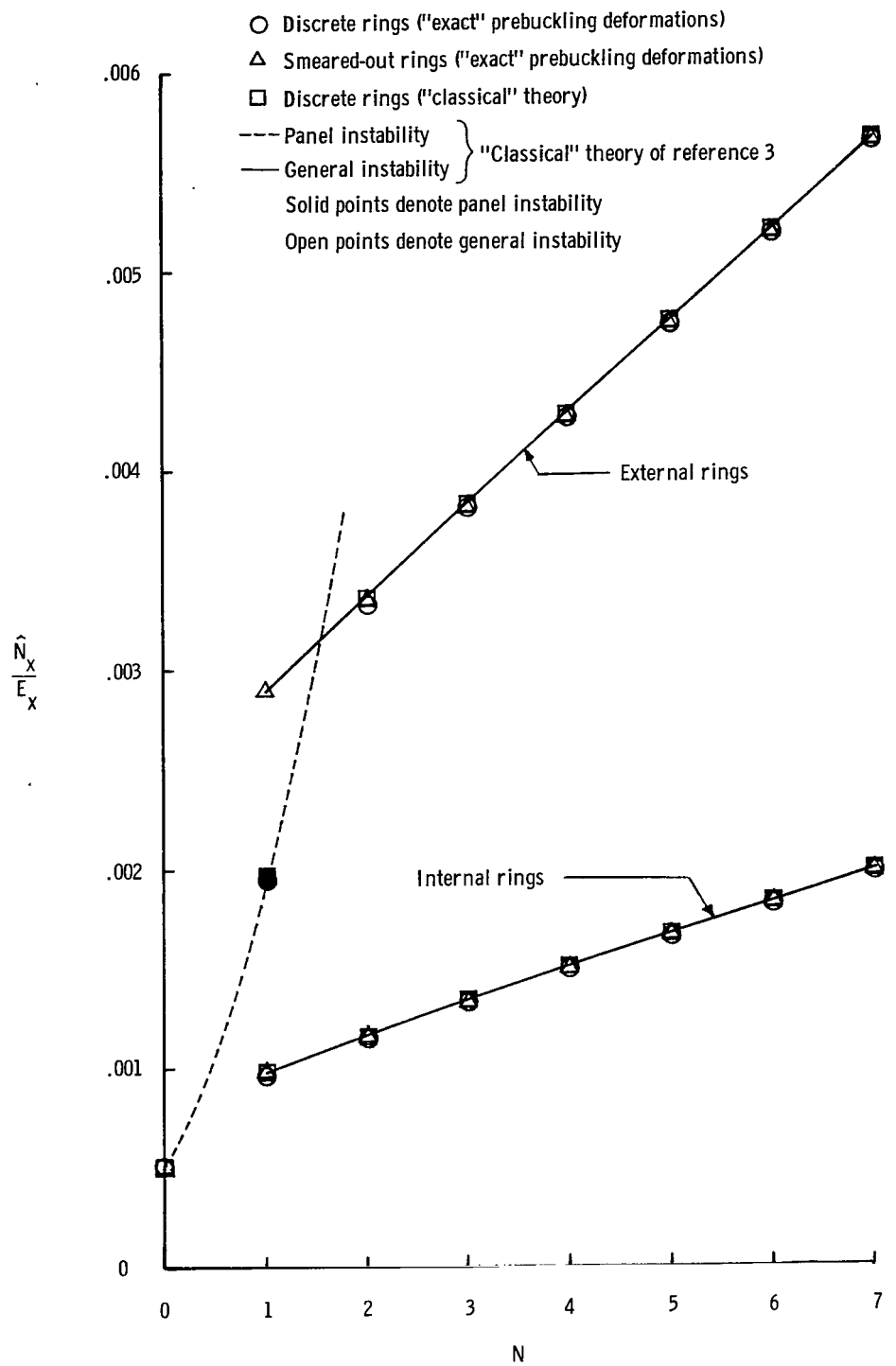

Figure 5.- Buckling predictions for simply supported axially compressed ring-stiffened corrugated cylinders.

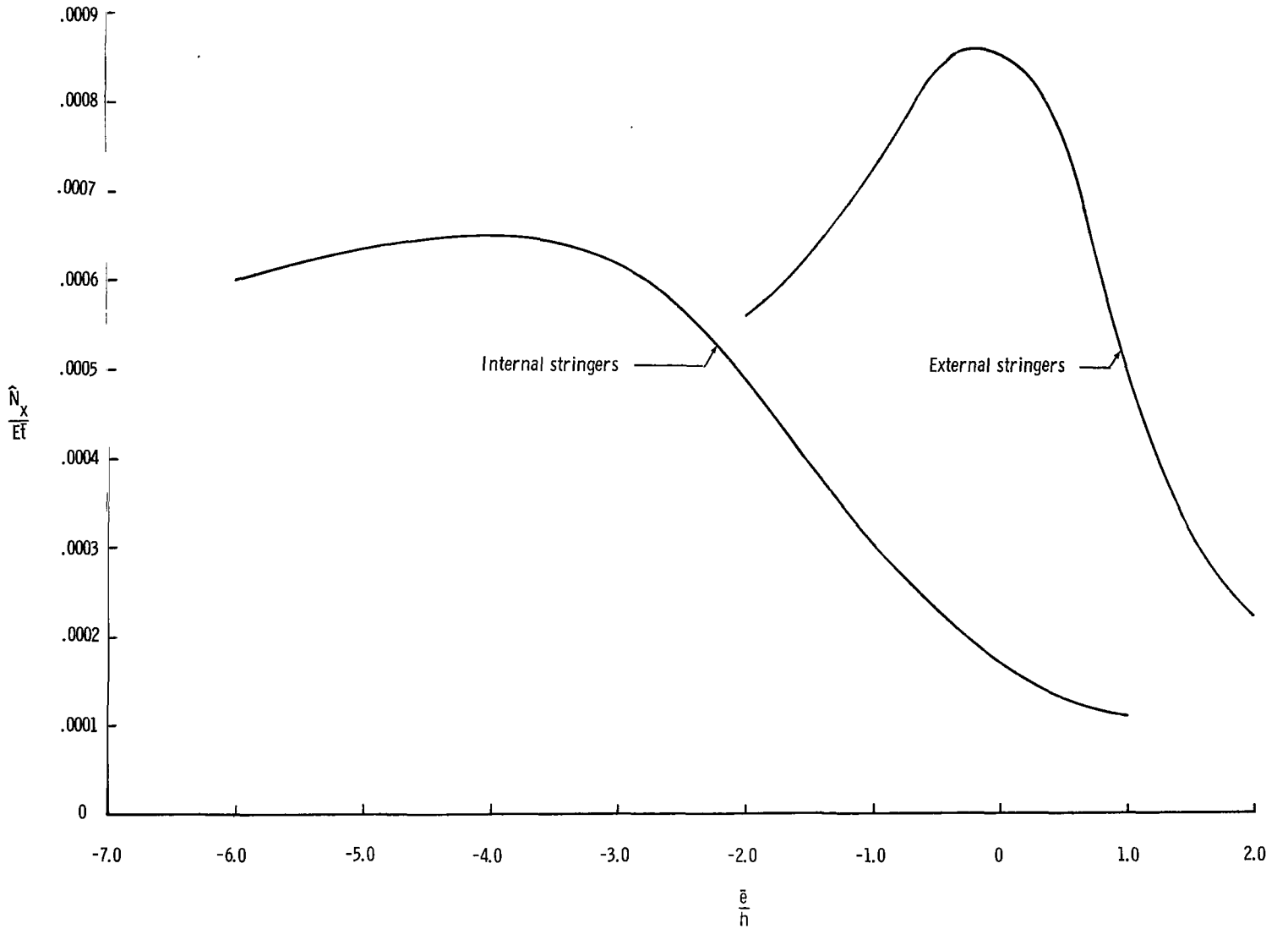

Figure 6.- Influence of eccentrically applied compressive loads on the buckling loads of simply supported stringer-stiffened isotropic cylinders.

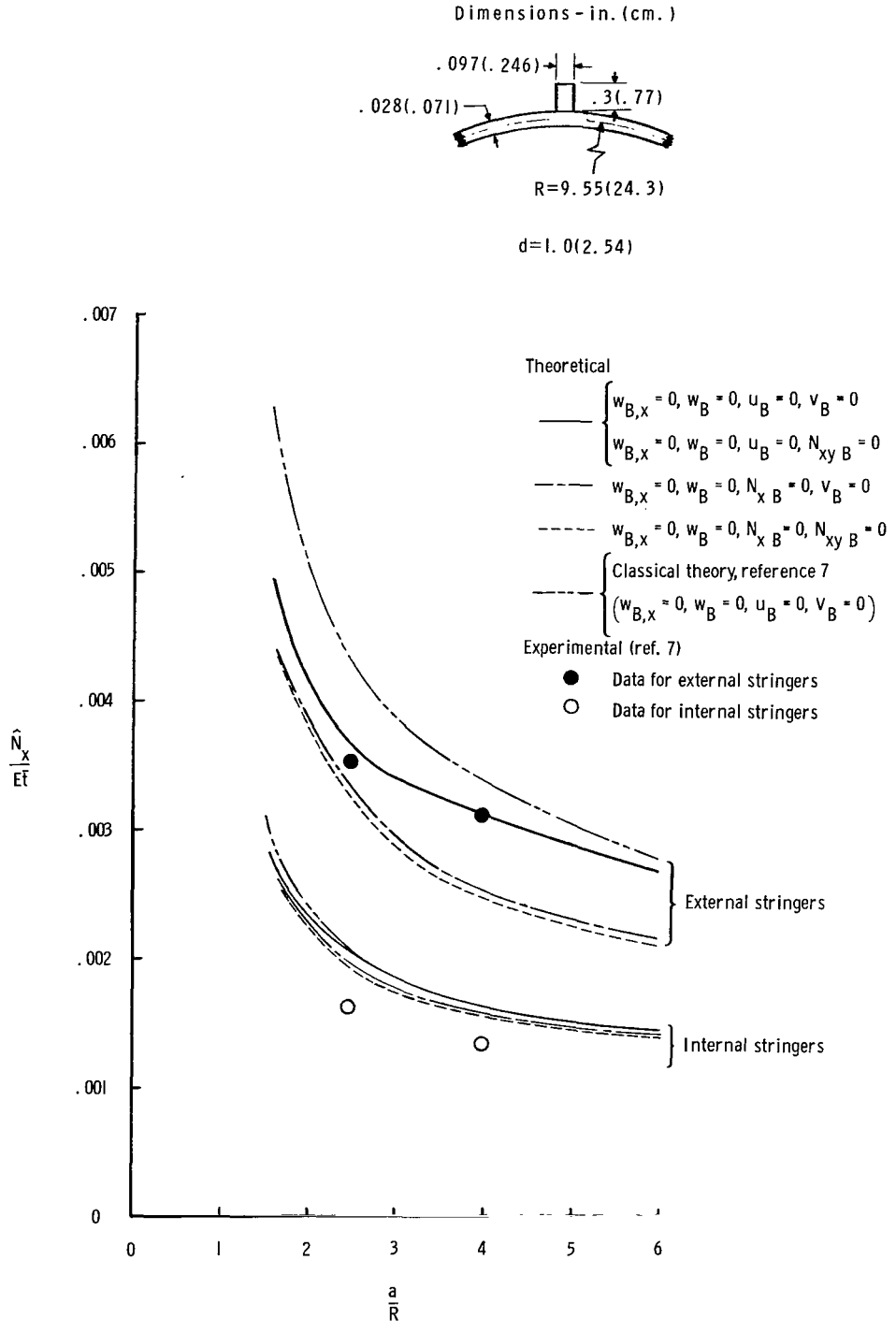

Figure 7.- Buckling of axially compressed integrally stiffened cylinders.

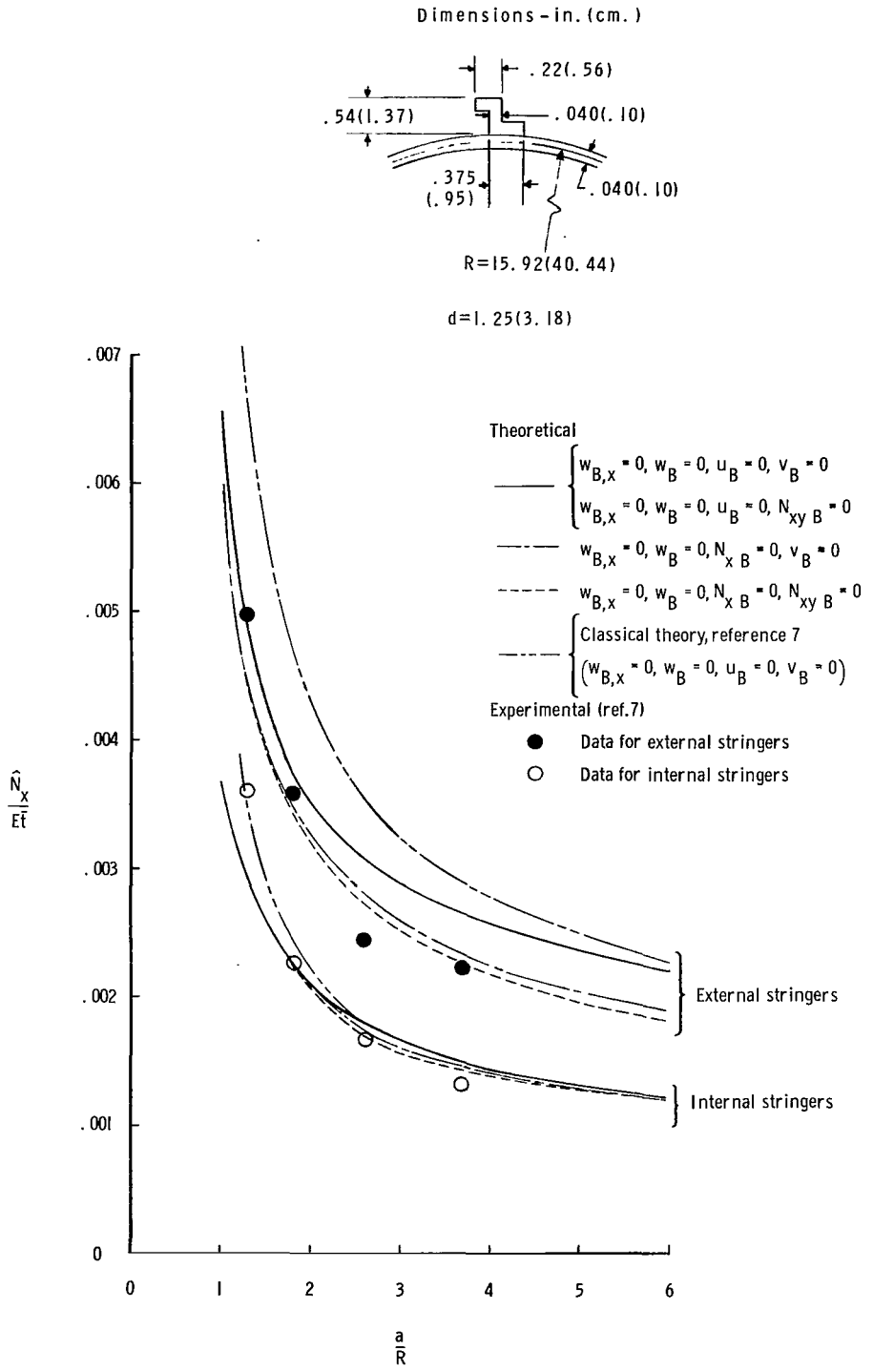

Figure 8.- Buckling of axially compressed Z-stiffened cylinders.

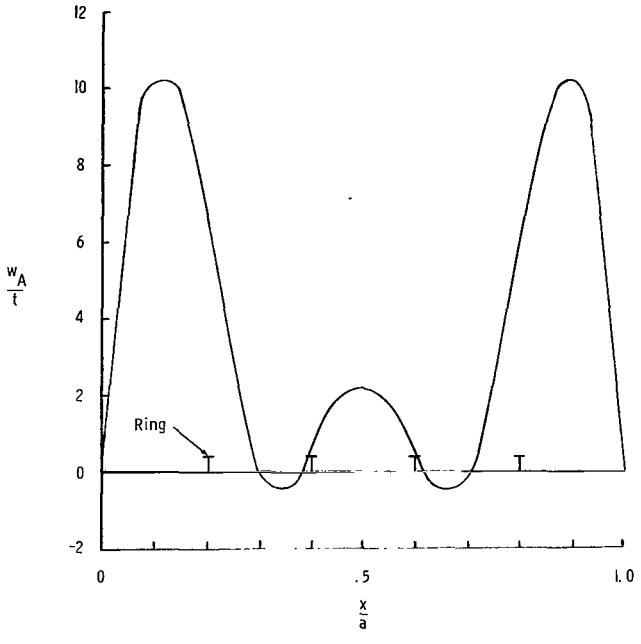

(a) Prebuckling shape; external rings and external stringers.

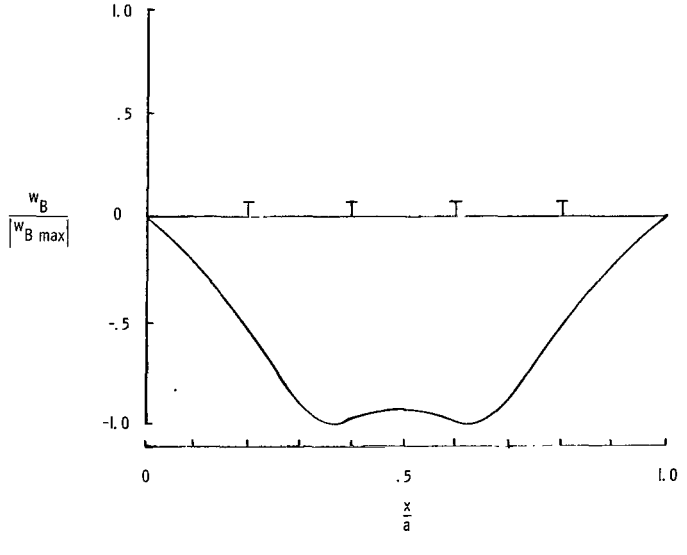

(b) General instability; external rings and external stringers.

Figure 9.- Prebuckling and buckling shapes of simply supported ring- and stringer-stiffened isotropic cylinders with four rings.

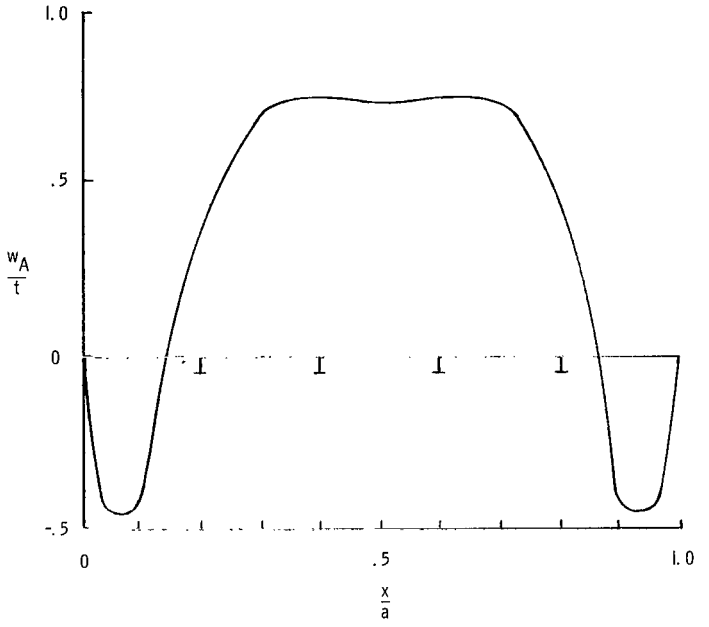

(c) Prebuckling shape; internal rings and internal stringers.

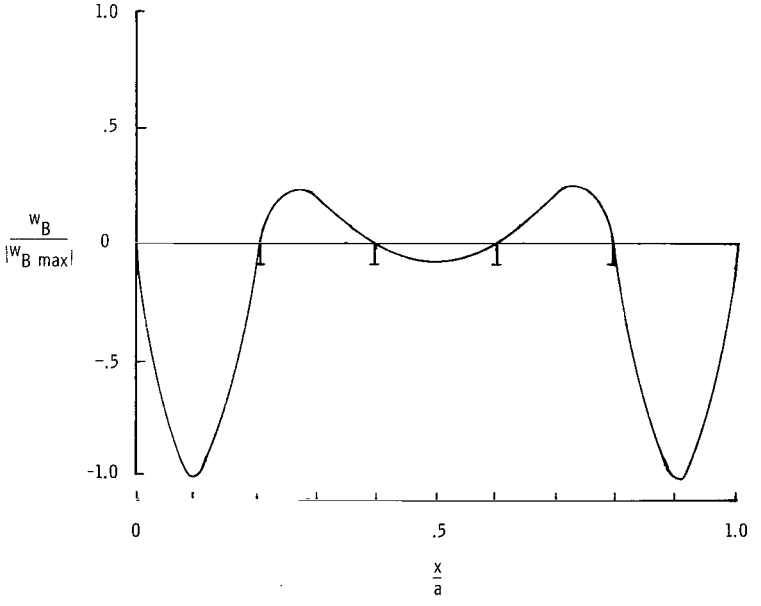

(d) Panel instability; internal rings and internal stringers.

Figure 9.- Concluded.

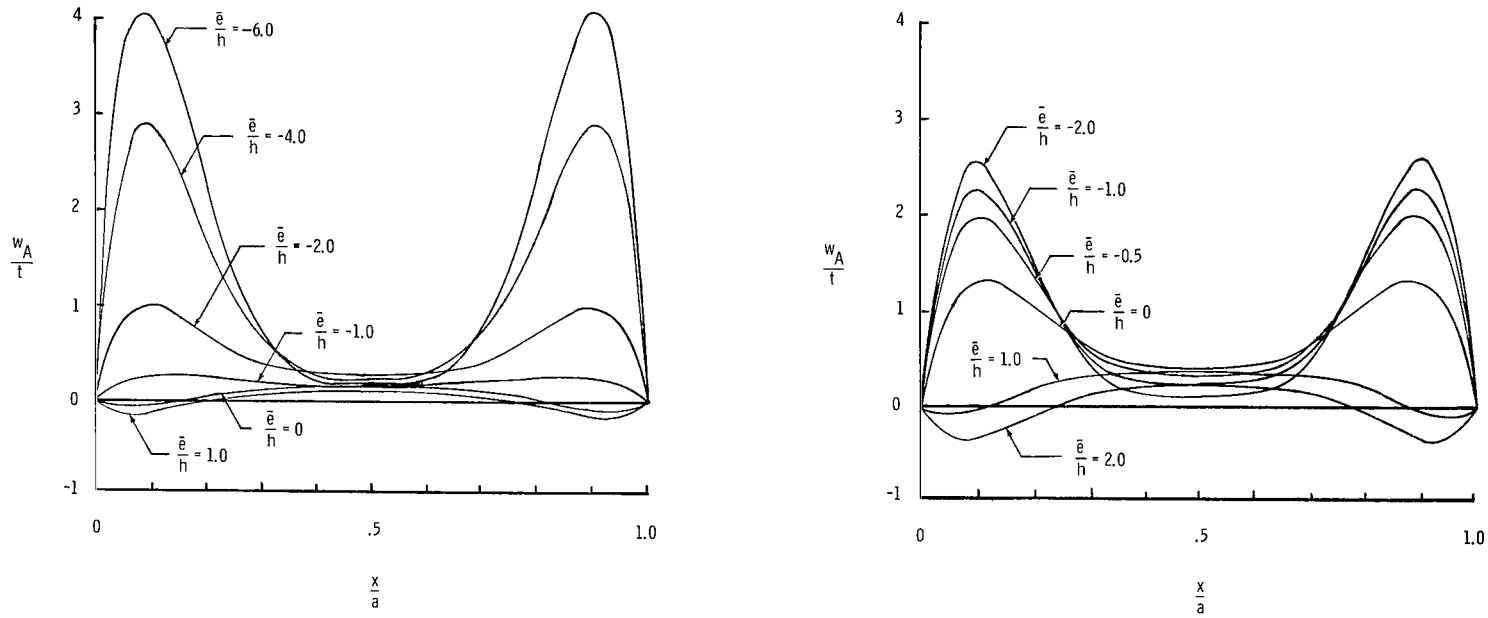

(a) Internal stringers.

(b) External stringers.

Figure 10.- Prebuckling shapes for simply supported stringer-stiffened isotropic cylinders with eccentrically applied compressive loads.

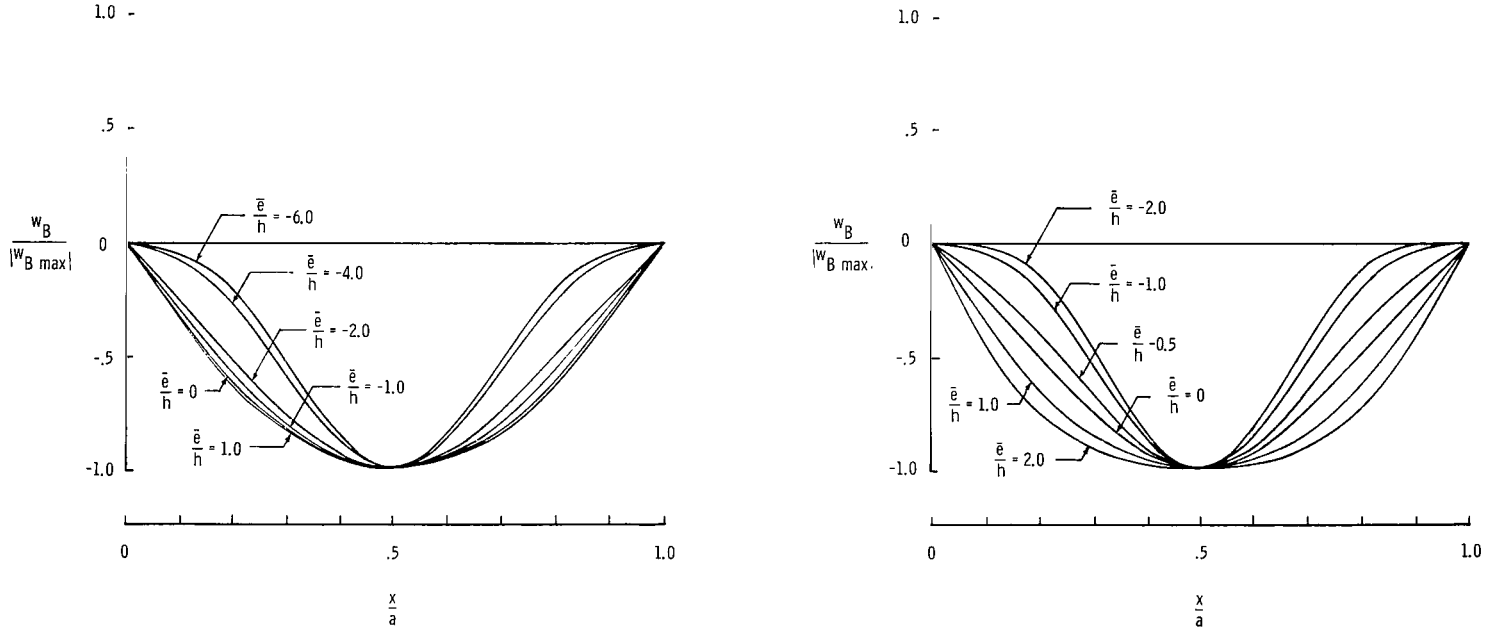

(a) Internal stringers.

(b) External stringers.

Figure 11.- Buckling shapes for simply supported stringer-stiffened isotropic cylinders with eccentrically applied compressive loads.

"The aeronautical and space activities of the United States shall be conducted so as to contribute . . . to the expansion of human knowledge of phenomena in the atmosphere and space. The Administration shall provide for the widest practicable and appropriate dissemination of information concerning its activities and the results thereof."

—NATIONAL AERONAUTICS AND SPACE ACT OF 1958

NASA SCIENTIFIC AND TECHNICAL PUBLICATIONS

TECHNICAL REPORTS: Scientific and technical information considered important, complete, and a lasting contribution to existing knowledge.

TECHNICAL NOTES: Information less broad in scope but nevertheless of importance as a contribution to existing knowledge.

TECHNICAL MEMORANDUMS: Information receiving limited distribution because of preliminary data, security classification, or other reasons.

CONTRACTOR REPORTS: Scientific and technical information generated under a NASA contract or grant and considered an important contribution to existing knowledge.

TECHNICAL TRANSLATIONS: Information published in a foreign language considered to merit NASA distribution in English.

SPECIAL PUBLICATIONS: Information derived from or of value to NASA activities. Publications include conference proceedings, monographs, data compilations, handbooks, sourcebooks, and special bibliographies.

TECHNOLOGY UTILIZATION PUBLICATIONS: Information on technology used by NASA that may be of particular interest in commercial and other non-aerospace applications. Publications include Tech Briefs, Technology Utilization Reports and Notes, and Technology Surveys.

Details on the availability of these publications may be obtained from:

SCIENTIFIC AND TECHNICAL INFORMATION DIVISION

NATIONAL AERONAUTICS AND SPACE ADMINISTRATION

Washington, D.C. 20546